Sour Tamarind Is More Antihypertensive Than the Sweeter One: Evidenced by the In Vivo Biochemical Indexes, Ligand-Protein Interaction, Multitarget Interactions, and Molecular Dynamic Simulation

Md. Atiar Rahman *, Taslima Akter, Rakibul Hassan Bulbul, Imran Sama-ae, Prof. M. A. Azadi, Kamrun Nahar Nira, Salahuddin Quader Al-Araby, Jobaier Ibne Deen, Khalid Juhani Rafi, Srabonti Saha, Md. Muzahid Ahmed Ezaj

Posted Date: 12 June 2023

doi: 10.20944/preprints202306.0819.v1

Keywords: Antihypertensive; Tamarindus indica; Gamma-sitosterol; troponin I; dynamic simulation; network pharmacology

Research paper

Sour Tamarind Is More Antihypertensive than the Sweeter One: Evidenced by the In Vivo Biochemical Indexes, Ligand-Protein Interaction, Multitarget Interactions, and Molecular Dynamic Simulation

Taslima Akter [1], Rakibul Hassan Bulbul [2], Md. Ali Azadi [4], Kamrun Nahar Nira [1], Salahuddin Quader Al-Araby [1], Jobaier Ibne Deen [1], Md. Khalid Juhani Rafi [1], Srabonti Saha [1], Md. Muzahid Ahmed Ezaj [5] and Md. Atiar Rahman [1,3,*]

[1] Department of Biochemistry and Molecular Biology, University of Chittagong, Chittagong–4331, Bangladesh.
[2] Institute for Developing Science and Health Initiatives, ideshi, Fouzderhat-4316, Chittagong
[3] School of Allied Health Sciences, Walailak University, Nakhon Si Thammarat, 80160, Thailand.
[4] Department of Zoology, University of Chittagong, Chittagong–4331, Bangladesh.
[5] Department of Genetic Engineering and Biotechnology, University of Chittagong, Chittagong–4331, Bangladesh
* Correspondence: Department of Biochemistry & Molecular Biology, University of Chittagong, Chittagong-4331, Bangladesh, Tel: +88-031-2606001-10, Extension- 4334, Fax: +88-031-726310, E-mail: atiar@cu.ac.bd and School of Allied Health Sciences, Walailak University, Nakhon Si Thammarat, 80160, Thailand; Cell: +66971174180

Highlights:

- *Tamarindus indica* displayed promising antihypertensive effects
- Sour tamarind conferred a higher antihypertensive effect than sweeter one
- Troponin I, C-reactive protein, and serum enzymes are excitingly normalized
- Gamma-sitosterol revealed by sour tamarind showed the best drug-likeliness
- Hub genes were strongly modulated by Gamma-sitosterol
- Binding of Gamma-sitosterol with target protein was most stable in biological system

Abstract : This research investigated the antihypertensive effects of tamarind products and compared their potentials based on their animal model's data verified by molecular docking, multitarget interactions in network pharmacology, and dynamic simulation assays. The GC-MS characterized tamarind products were administered to the cholesterol-induced hypertensive Wistar albino rat models. Two-week-intervened animals were dissected to collect serum and organs which were respectively subjected to the analyses of hypertension-linked markers and tissue architectures. Lead biometabolites of tamarinds interacted with eight target receptors in molecular docking and dynamic simulation studies and they were tested for multitarget interactions using network pharmacological analyses. Results showed that serum alanine aminotransferase (ALT), aspartate aminotransferase (AST), alkaline phosphatase (ALP), C-reactive protein (CRP), Troponin I, and lipid profiles were maximally reinstated by the phenolic-enriched ripened sour over the sweet tamarind flesh extracts, but seed extracts had a smaller influence. Among the tamarind's biometabolites, Gamma-sitosterol (ϒ-sitosterol) was found to be the best ligand in managing hypertension via the possible ligand-receptor interactions with the guanylate cyclase which displayed the best drug-likeliness through the highest binding energy -9.3 Kcal. Multitargeted interactions-based degree algorithm and phylogenetic tree of pathways showed 14 targeted genes, of which *NR3C1, REN, PPARG, and CYP11B1* hub genes, were consistently modulated by the ϒ-sitosterol to reduce hypertension and related risk factors. The dynamic simulation study showed that the P-RMSD values of ϒ-sitosterol-guanylate cyclase were stable between 75.00 to 100.00 ns at the binding pocket. The findings demonstrate that ripened sour tamarind extract may be

supplemented to be a more prospective antihypertensive target or nutraceuticals affirming through advanced preclinical and clinical studies.

Keywords: Antihypertensive; *Tamarindus indica*; Gamma-sitosterol; troponin I; dynamic simulation; network pharmacology

Introduction

Hypertension is a major risk factor for cardiac disease and stroke, with an increase in risk for these ailments with progressively higher blood pressure, dyslipidemia, and obesity. The total lipid profile of an individual is a contributive principle resulting from blood cholesterol along with its associated varieties of lipoproteins i.e., high-density lipoproteins (HDL, or α-lipoproteins), low-density lipoproteins (LDL, or β-lipoproteins), Very-low density lipoproteins (VLDL, or pre-β-lipoproteins) and Triglycerides. Disposition of blood pressure and coronary heart diseases to be in strong correlation with lipid profile, particularly with blood cholesterol level [1].

The interrelationship between liver dysfunction and the development of hypertension is being increasingly recognized. The liver is a vital organ in metabolism that plays numerous roles including synthesis, degradation, storage, and biotransformation of biomolecules in the human body [2]. The liver enzymes alanine and aspartate aminotransferase (ALT and AST), γ-glutamyltransferase (GGT), and alkaline phosphatase (ALP) have been widely used as good markers of liver health, some epidemiological studies have demonstrated an association of ALT and GGT with metabolic syndrome, CVD and type 2 diabetes [3].

The contraction of smooth muscle cells is thought to be related to a rise in intracellular calcium concentration, which may explain the vasodilatory effect of calcium channel-blocking drugs. Prolonged contraction of SMC is thought to induce structural changes with thickening of the arteriolar vessel walls possibly mediated by angiotensin, leading to an irreversible rise in peripheral resistance. Cardiac output is related to sympathetic overactivity [4].

Phytochemicals are mainly classified into flavonols, flavones, flavanones, isoflavones, catechins, anthocyanidins, and chalcones. The common feature of flavonoid compounds is their phenyl benzopyrone skeleton (C6-C3-C6) [5,6] and they are antioxidants that often function as reducing agents such as thiols, ascorbic acid, or polyphenols. They exist as vitamins, minerals, and other compounds in foods [6]. The antioxidant property is mainly brought about by the presence of polyphenolic compounds such as anthocyanins, flavonoids, phenolic acids, and phenolic diterpenes. *T. indica* L. is said to contain a large number of polyphenolic compounds with the potential for antioxidant activity [7].

For the treatment of cardiovascular diseases, including hypertension, modern medical science has developed several synthetic drugs and therapeutics with improved efficacy, but they possess a significant number of side effects. Herbal medicines, therefore, have been regaining importance because of their ease of availability, fewer side effects, and cost-effectiveness [8]. Ethnobotanical surveys of various medicinal plants indicate their vast use in the treatment of cardiovascular disorders. For example, plants like Syzyiumglineens, *Tamarindus indica*; *Passiflora nepalensis* wall, etc. have been used for the treatment of hypertension [9].

Tamarindus indica, a Fabaceae family member, also referred to as tamarind, is frequently used in traditional cooking and Ayurvedic herbal remedies. According to numerous studies, *T. indica* is a multifunctional tree, with every part of the tree having at least some nutritional or therapeutic benefit. Proanthocyanidins, an oligomeric flavonoid also known as condensed tannins, which are used as powerful antioxidants and are usually present in the peels of fruits and vegetables, are among the phenolic antioxidants present in the tamarind pericarp[17]. In different parts of Bangladesh, there are various varieties of tamarind, especially sour and sweet types, but the full extent of their health benefits has not yet been discovered. Akter et al. (2022) have recently reported the cardioprotective role of sour tamarind while the sweeter one is unaddressed [10]. Considering the foregoing, the

 doi:10.20944/preprints202306.0819.v1

current investigation was undertaken to assess the antihypertensive effects of different types of *T. indica* extracts on cholesterol-induced hypertensive Wistar albino rats. The results were further verified by the comprehensive computational biological study using target-ligand receptor interactions, and network-pharmacological and biological simulation assays.

Materials and methods

2.1. Chemicals and reagents

All reagents used in this investigation were of analytical grade until explicitly described. Cholesterol (CAS No: 57-88-5) was purchased from Sigma-Aldrich (St. Louis, MO), Avastrol (Atorvastatin) (Albion Laboratories Ltd., Bangladesh), Methanol (CAS No: 67-56-1), Hydrochloric acid (CAS No: 7647-01-0), Sodium hydroxide (CAS No: 1310-73-2), Aluminum chloride (CAS No: 7446-70-0), Sodium carbonate (CAS No: 497-19-8), Potassium ferricyanide (III) (CAS No: 13746-66-2), Iodine (CAS No: 7553-56-2), and Potassium iodide (CAS No: 7681-11-0) were purchased from Sigma-Aldrich (St. Louis, MO). Folin–Ciocalteu reagent, gallic acid (CAS No: 149-91-7), vanillic acid (CAS No: 121-34-6), rutin (CAS No: 153-18-4), and catechin (CAS No: 154-23-4) were also purchased from Sigma-Aldrich (St. Louis, MO).

2.2. Collection of sample material

Sour and sweet *Tamarindus indica* fruits were used as samples in this investigation. Sour *T. indica* fruits were collected from the local market of Chittagong University (GPS: 22.479827, 91.793494) and sweet varieties of *T. indica* were collected from the local Barmiest market of Cox's Bazar (GPS:21°25′38″N 92°00′18″E). The samples were authenticated as *T. indica* by Dr. Shaikh Bokhtear Uddin, Taxonomist, and Professor, Department of Botany, University of Chittagong. The voucher specimen for the samples were preserved as the accession numbers (sour variety-CAMH19/03, sweet variety-BCAMH19/04).

2.3. Preparation of extract from the flesh of Tamarind

Immediately after the collection of *T. indica*, the skin of the fruits was removed, and the fleshy pericarp and hard seeds were separated from each other. Tamarind fleshes were then mixed with water and pulverized by a mechanical blender machine (Sonipat, Heavy Duty Electric Dry Masala & Herbs Grinder, Swing Type 2300W Haryana, India) to make a juicy extract of tamarind and seeds of ripened sour Tamarind were dried and ground with an irony mortar and pestle. The crushed seeds were then mixed with water to make the aqueous extracts of the seeds. All the extracts were filtered by cheese clothes and then keep it in an incubator at 45°C temperature. The crudes of different semisolid extracts of tamarind parts were henceforth known as Flesh of Ripen Sour Tamarind = FRiST; Seed of Ripen Sour Tamarind = SRiST; Flesh of Raw Sour Tamarind = FRaST; Flesh of Sweet Tamarind = FSwT to preserve them Eppendorfpendorf tube covered by parafilm, and put to sieves on the cap of the tube. After 3 days of refrigeration at -80 °C, the sample was lyophilized by a freeze drier Labconco (Labcono 7934000, Kansas City, MO, USA). The lyophilized sample was stored at -40 °C for future use.

2.4. Standardization of the extraction procedure

An established method was used to optimize the crude extraction process [11]. The dried materials were quickly extracted using water at 23 ± 0.5°C. A central composition design was used to assess the impact of the two factors, extraction time (T: 36-72 h), and solvent-sample ratio (SSR: 2/1 to 4/1) represented as milliliters of solvent per gram of dried material. The solvent was evaporated from the extract using a vacuum evaporator (RE 200, Bibby Sterling Ltd.) and filter paper (Whatman # 1).

 doi:10.20944/preprints202306.0819.v1

2.5. Screening for phytochemical content of prepared aqueous extracts

2.5.1. Determinations of total flavonoid content (TFC), total phenolic content (TPC), total proanthocyanidin content (TPrAC), and total antioxidant capacity (TAC) of FRiST, SRiST, FRaST, and FSwT

The total flavonoid content (TFC) of the aqueous extracts was determined according to the method established by Kumaran and Karunakaran et al. (2007) [9]. The total phenolic content (TPC) of the four samples of tamarinds was measured according to a method described by Singleton and Rossi et al. (1965) [12]. Quantitative estimation of proanthocyanidins (TPrAC) and total antioxidant (TA) capacity were carried out using the modified HCl-Vanillin method established by Abdelseed et al. 2011 [13].

2.6. GC-MS analysis of FRiST and FSwT

The crudes of FRiST and FSwT were analyzed by GC-MS using electron impact ionization (EI) with a gas chromatograph (GC-17A, Shimadzu Corporation, Kyoto, Japan) coupled to a mass spectrometer (GC-MS TQ 8040, Shimadzu Corporation, Kyoto, Japan). A fused silica capillary column (Rxi-5ms; 0.25m film thickness) is coated with DB-1 (J&W). The inlet temperature of the capillary was set at 260°C and the oven temperature was set at 70°C (0 min); 10°C, 150°C (5 min); 12°C, 200°C (15 min); 12°C, 220°C (5 min). The column flow rate was 0.6 mL/min Helium gas at a constant pressure of 90 KPa. The auxiliary (GC to MS interface) temperature was set at 280°C. The MS was set in scan mode with a scanning range of 40-350 amu. The mass range was set in the range of 50–550 m/z. The prepared sample was then run for GC/MS analysis. The total GC-MS running time was 35 min. All peak areas were compared with the database in the GC-MS library version NIST 08-S.

2.7. Qualitative identification of carbohydrates, proteins, alkaloids, glycosides, tannins, saponins, phenolic compounds, steroids, triterpenoids, and flavonoids

The presence of carbohydrates was determined by Fehling's test, Fehling's A, and Fehling's B reagent. The presence of protein, alkaloid, glycoside, tannins, saponins, phenolic compounds, steroids, and triterpenoids was tested by the Biuret test, Wagner's test, Glacial acetic acid test, lead acetate test, Saponins test, Salkowski's test and Alkaline reagent test respectively [14,15].

2.8. Experimental animals and their maintenance

The antihypertensive activity of the extract was carried out on 38 male Wistar albino rats aged 6-8 weeks (average weight, 150–200 g) before the experiment. Animals were housed in standard environmental conditions under a 12/12 h light/dark natural cycle in the animal house of the Department of Biochemistry and Molecular Biology, University of Chittagong. The animals were individually housed in a polycarbonated cage bedded with wood husk at a temperature of 22 ± 2 ºC and humidity of 55–60%. All animals had free access a to standard diet and tap water. The ARRIVE ethical guidelines-based approval from the Ethical Review Board of the Faculty of Biological Sciences, University of Chittagong, verified the animal care, dosing, and sacrifice (AERB_FBSCU_20230213(6)).

2.9. Induction of hypertension using cholesterol

Experimental Wistar albino rats (Age: 7-8 weeks, body weight: 180-200 g) of either sex were randomly divided into control and treatment groups comprising 4 animals in each group. The negative control group received vehicles only. The hypertensive control group was left untreated. The treatment groups were administered with two different doses (50 mg and 100 mg/kg BW) of FRiST, SRiST, FRaST, and FSwT aqueous extracts. Groups except those of negative control groups were fed with cholesterol (150 mg/kg BW) dissolved in vegetable oil to induce hypertension. Meanwhile, eight treatment groups are treated with aqueous extracts of FRiST, SRiST, FRaST, and FSwT each at the dose of 50 mg/kg and 10 mg/kg BW. The treatment was continued for 14 days.

Preprints (www.preprints.org) | NOT PEER-REVIEWED | Posted: 12 June 2023 doi:10.20944/preprints202306.0819.v1

2.9.1. Recording the animal's body weights and collection of blood and organs

Body weights of the intervened animals were recorded each week and treatments were provided by feeding needle. Animals were sacrificed after two weeks of intervention, and their blood, liver, and hearts were taken in heparinized test tubes. Blood samples were centrifuged at 3000 rpm for 15 min at 20°C to separate serum which was further analyzed for biochemical analyses. The liver and heart were collected from each animal and washed with 0.9% NaCl (normal saline). The organs were then wiped with tissue paper and weighed. The weighed organs were preserved with 4% buffered formalin within the plastic vials. The weights of the liver, and heart were recorded. The liver was used to determine glycogen level. Hearts were used for histopathological investigation. Liver glycogen concentrations were measured by a phenol-sulfuric acid method as described by [14].

2.9.2. Biochemical analyses of serum

Serum biochemical parameters including Aspartate aminotransferase–AST, Alanine aminotransferase–ALT, Alkaline Phosphatase–ALP, lipid profile, Troponin I, C-reactive protein-CRP, creatinine kinase (CK-MB), lactate dehydrogenase (LDH), creatinine levels were measured by using reaction kits onsemi-autoanalyzerser (Humalyzer 3000, Human).

2.9.3. Liver glycogen estimation

Determination of hepatic glycogen was performed by the phenol-sulfuric acid method as described by Lo et al., (1970) [14]. The standard-1 solution, which was generated at a concentration of 1000 g/mL, was diluted four more times to create the standard-2 (500 g/mL), standard-3 (250 g/mL), standard-4 (125 g/mL), and standard-5 (62.5 g/mL) solutions. These were the standard solutions for this experiment. The liver samples (about 80 mg) were transferred to test tubes containing 30% KOH (w/v), which was saturated with Na_2SO_4. The liver tissues dissolved in KOH were then boiled for 30 min until complete homogenization occurs. The homogenized mixture was cooled in ice. Glycogen was precipitated by adding 2 mL 95% ethanol and then incubated on ice for 30 min. The test tubes were then centrifuged at 840 g (3000 rpm) for 20-30 min. The supernatants were discarded, and the precipitate was dissolved in 3 mL distilled water and an aliquot was then diluted 1:4 (100 µL aliquot in 400 µL distilled water). Standard was also started from here. Both the sample and standards were run in duplicate. One mL of 5% phenol and then of 5 mL 96 % H_2SO_4 were added to the solution and stood for 10 min. The solutions were incubated at 25 – 30 °C for 15 min. Absorbances (OD) of the solutions were measured at 490 nm. Glycogen concentrations of tissues were calculated using the following equation [14].

$$\textbf{Liver glycogen (mg/g tissue)} = \mathbf{A/k \times V/v \times 10^{-4}/w}$$

Here,

k = slope of the standard curve,
V = total volume (ml) of glycogen solution,
v = volume (ml) of aliquot to which phenol-sulfuric acid solution is added,
A = absorbance at 490 nm,
w = sample weight (g).

2.9.4. Histopathological analyses

Immediately after sacrifice, the tissues were collected and preserved at 4% buffered formalin for 48 h. The formalin was changed every week until the Histopathological analysis had been done. The vertical sections of tissues were taken by sharp blade for further processes. The tissues were dehydrated by passing through ascending grades of ethanol 70%, 80%, 90%, 100% vol/vol) for one h in each solution. The tissues were passed through 100% ethanol three times, for a total of 3 h. Here samples were transferred through progressively more concentrated ethanol to remove the water from the tissue. To remove alcohol from the tissues. The tissues were passed through the xylene solution three times consecutively for of total three h, one h per xylene solution. The tissues were then

 doi:10.20944/preprints202306.0819.v1

embedded in molten Paraffin wax. the tissue samples were placed into molds along with paraffin, then allowed to be cooled and hardened, and preserved at 4 °C until cross-section was done. The embedded tissues were sectioned at 5 µm using a semi-automated rotator microtome (Biobase Bk-2258, Laboratory Manual Microtome, China). The tissue sections were then mounted on glass slides using an incubator at 60-70 °C for 30 min. Afterward, the tissue sections were deparaffinized with xylene and rehydrated by using different graded ethanol dilutions (100%, 90%, and 70%). The sections were stained with hematoxylin and Eosin (H & E). All slides of the liver and heart were examined under Olympus BX51 Microscope (Olympus Corporation, Tokyo, Japan), and the histopathological images were taken with the help of the Olympus DP20 system under a magnification of X200.

2.10. Statistical analysis

All data are presented as a mean ± standard error of the mean. The data were analyzed by statistical software statistical package for social sciences (SPSS, Version 22.0, IBM Corporation, NY) using one-way analysis of variance (ANOVA) followed by Tukey's post hoc tests for multiple comparisons. The values were considered significantly different at $P < 0.05$.

2.11. In silico approaches

2.11.1. Molecular docking analysis

Based on a review of the literature, the receptors/enzymes were chosen for molecular interaction to reveal anti-hypertensive activity [15–17]. The 3D crystal structures of Tyrosine Hydroxylase (PDB ID: 1TOH), BETA-1 subunit of the soluble guanylyl cyclase(PDB ID: 3HLS), Human High-conductance Ca^{2+} gated K^{+} Channel (BK Channel)(PDB ID: 3NAF), Nuclear hormone receptor PPAR-gamma (PDB ID: 3R8 A), Human Angiotensin Receptor(PDB ID: 4Y AY), Macrocyclic IL-17A antagonists (PDB ID: 5H I3), Human soluble guanylate cyclase (PDB ID: 6JT0) were imported from the RCSB Protein Data Bank (PDB), an online database (https://www.rcsb.or g/). The Discovery Studio protein preparation protocol was used to accomplish tasks such as inserting missing atoms into incomplete residues and removing water molecules, and ligands from proteins. Before processing, hydrogen atoms were also introduced to the protein molecules. Best binding sites were selected by using an online tool PockDrug [18]. The PubChem repository (https://pubchem.ncbi.nlm.nih.gov/) was used to extract the chemical structure of the main identified compounds from *T. indica* using GC-MS. The molecular docking research followed Hossen et al.'s methodology and was briefly described [19].

2.11.2. Evaluation of pharmacokinetic parameters

Lipinski's rule of fives [20] and Veber's rules (number of rotatable bonds; topological polar surface area) were used to assessing the absorption, distribution, metabolism, excretion, and toxicity (ADME/T) characteristics of bioactive compounds from AOME [21]. QikProp (Schrödinger Release 2017-1: QikProp, Schrödinger, LLC, New York, NY, USA) and SwissADME (http://www.swissadme.ch/) were used to evaluate the ADME/T properties. QikProp and SwissADME a powerful ADME/T prediction tool that predicts whether a compound's ADME/T performance will be acceptable.

2.11.3. Determination of toxicological properties

The AdmetSAR online tool was used to establish the toxicological properties of the selected compounds, as toxicity is a major worry during the development of novel drugs [22]. The Ames toxicity, carcinogenic properties, acute oral toxicity, and acute rat toxicity were all predicted in this research.

 doi:10.20944/preprints202306.0819.v1

2.12. Building the bioactive compound-target protein network

Target proteins associated with bioactive phytochemicals were discovered using SwissTargetPrediction (http://www.swisstargetprediction.ch/), which is based on network pharmacology-based prediction. Each pair of protein-chemical interactions receives a score. To match their possible targets, bioactive compounds (eight for GC-MF and all compounds for LC-MS-MS) were entered into SwissTargetPrediction collectively. The organism chosen was "Homo sapiens," and the median necessary interaction score was set at 0.4. We also utilized GeneCard (https://www.genecards.org), which predicts the matching possible bioactive targets with a probability greater than 0.1 for hypertension. Further investigation did not consider compound targets with no connection to the interactions between compounds and proteins. The target genes of the Swiss TargetPrediction and GeneCard were compared using the online application "Calculate and build custom Venn diagrams" (http://bioinformatics.psb.ugent.be/webtools/Venn/).

2.12. Development of the anticipated genes' protein-protein interaction (PPI) networks

By using the Search Tool for the Retrieval of Interacting Genes (STRING) database (https://string-db.org/cgi/input.pl; STRING-DB v11.0), we created a PPI network of the predicted genes. Using the Cytoscape plugin cytoHubba, the rank of the target proteins was determined based on the strength of connections in the PPI network. To create a PPI protein interaction network, the collected protein interaction data of the target proteins were imported into the Cytoscape 3.9.1 program.

2.13. Pathway enrichment analysis of the target proteins using Gene Ontology (GO) and the Kyoto Encyclopedia of Genes and Genomes (KEGG)

The Database for Annotation, Visualization, and Integrated Discovery (DAVID, https://david.ncifcrf.gov/) v6.8 was used to determine the function of target proteins that interact with the active components in gene function and signaling pathway. The projected genes were substantially related to the KEGG pathways, which were found. We examined the KEGG pathway enrichment and Gene Ontology (GO) function of identified genes. The target proteins connected to the KEGG pathways, cellular components (CC), molecular function (MF), and biological process (BP) were also characterized. A p-value of 0.05 or below was regarded as significant.

2.14. Molecular dynamics (MD) simulations

The MD simulations of the Thermolysin-gamma-sitosterol complex utilized the Schrödinger suite's Desmond module [23]. Hydrogen bonds were allocated using standard protocols throughout this process. The Thermolysin-gamma-sitosterol complexes were then subjected to the optimal potentials for liquid simulations (OPLS) force field. After immersing the complexes in a transferable intermolecular potential with 3 points (TIP3P) water model at a distance of 10 from the center of the box, the energy of the complexes was reduced. After then, the system was neutralized by adding sodium and chloride ions to simulate the in vivo environment. Next, molecular dynamic simulations were run for 100 ns with ensembles of constant numbers of particles, pressure, and temperature (NPT) with a recording interval of 100 ps [24]. The temperature and pressure were adjusted to 310.15 K and 1.01325 bar, respectively, to simulate the in vivo environment [25]. The simulation interaction diagram tool from Desmond Schrödinger's module was used to investigate the results [23].

Results

3.1. Phytochemical screening

Identification test for the carbohydrate, protein (biuret test), alkaloid, tannin (lead acetate test), Saponins (saponins test), steroids, and triterpenoids (Salkowski's test), Polyphenols and flavonoid (alkaline reagent test) had shown positive result indicating the presence of those phytochemical constituents in aqueous extracts of the pericarp of ripening sour *T. indica* (FRiST). On the other hand,

Preprints (www.preprints.org) | NOT PEER-REVIEWED | Posted: 12 June 2023 doi:10.20944/preprints202306.0819.v1

the test for the glycoside bond showed a negative result for the aqueous extracts of FRiST. The result is also figured in **Table 1**.

3.2. TFC, TPC, TPrAC, TAC of FRaST, First, FSwT, and SRiST extracts

The TFC was estimated by the standard rutin curve ($y = 0.002x + 0.174$, $R^2 = 0.426$)) and expressed as rutin equivalents per gram of the plant extract. The TFC of the four different samples was found to be 95.33 mg rutin/g for First, and FRaST, 115.5 mg rutin/g for FSwT, and 173.8 mg rutin/g for SRiST. Among the 4 samples, SRiST possesses the highest quantity of TFC. While TPC using the Folin-Ciocalteu reagent method was found to be 0.15 mg GAE/µg for sample FRiST, 0.24 mg GAE/µg for both FRaST and FSwT, and 0.063 mg GAE/ µg for the TB. The TPrAC of four *T. indica* extracts was found to be 2.663 mg/g of dry weight for FRiST, 15.4 mg/g dry weight for FRaST, 4.55 mg/g dry weight for FSwT and 8.44 mg/g dry weight for SRiST respectively. The data has been shown that water might not a good extract for proanthocyanidin elucidation. The data are presented in **Table 2**. #

Table 1. Phytochemical screening of *Tamarindus indica.*

Tests	Biochemical test	Observation	Result
Carbohydrate	Fehling's test	Brick-red PPT	+
Protein	Biuret test (Piotrowski's test)	A purple color	+
Alkaloid	Wagner's test	Reddish-brown PPT	+
Glycoside	Keller-Kiliani Test	No color formation	-
Tannins	Lead acetate test	White PPT	+
Phenols	Lead acetate test	White PPT	+
Saponins	Froth test	Froth formation	+
Steroids	Salkowski's test	Red color	+
Terpenoids	Salkowski's test	Reddish brown color	+
Flavonoids	Alkaline Reagent Test	Light Yellow color	+
Sterol test			0

PPT = Precipitate formation, froth = Presence of froth in the test tube. (+) = present, (-) = absent.

Table 2. Total flavonoid content (TFC), total phenolic content (TPC), total proanthocyanidin content (TPrAC), and total antioxidant capacity (TAC) of different parts of *Tamarindus indica* fruit aqueous extract (TIFAE).

Parts of TIFAE	TFC, RE (mg/g)	TPC, GAE (mg/g)	TPrAC, Catechin (mg/g)	TAC, Catechin (mg/g)
FRiST	95.33 ± 1.39	185.81 ± 0.55	26.63 ± 0.09	62.91 ± 2.46
SRiST	173.76 ± 0.74	63.54 ± 0.22	84.41 ± 4.98	56.66 ± 1.46
FRaST	133.50 ± 1.17	236.16 ± 0.60	153.86 ± 1.97	62.91 ± 0.97
FSwT	115.47 ± 0.56	240.94 ± 0.52	45.52 ± 1.48	181.63 ± 1.78

Each value in the table is represented as mean ± SD for n = 3; FRiST = Flesh of Ripen Sour Tamarind; SRiST = Seed of Ripen Sour Tamarind; FRaST = Flesh of Raw Sour Tamarind; FSwT = Flesh of Sweet Tamarind; TFC = mg rutin equivalents (RE) per g of dried fruit/seed; TPC = mg gallic acid equivalents (GAE) per mg of dried fruit/seed; TPrAC = mg catechin equivalents per g of dried fruit/seed; TAC = mg catechin equivalents per g of dried fruit/seed.

3.3. Effect of the tamarind products on the body and organ weights of experimental animals

Positive control (PC, atenolol) and all the treatment groups except SRiST100 were noticed to inhibit gaining weight of animals while normal control groups showed a significant ($P < 0.05$) increase in body weight (**Table 3**). The cholesterol was found to induce the rats to weight gain whereas the reference control and the treatment of FRiST50, FRiST100, FRaST50, FRaST100, and FSwT100 were shown to effectively inhibit the gaining of animal body weight. However, the weight gain of the

Preprints (www.preprints.org) | NOT PEER-REVIEWED | Posted: 12 June 2023 doi:10.20944/preprints202306.0819.v1

SRiST100 group was insignificant in comparison to compared to NC groups. The sour and sweet tamarinds equally contributed to protecting the liver and heart weights of experimental animals. The FSwT50 & 100 and FRiST50 & 100 were recognized to significantly improve the liver weight compared to the positive control while the same doses were noticed to reduce the heart weight significantly implying their consistent effect in the antihypertensive role. Figure 1 displayed the comparative relative weights of the liver heart and heart of the intervened animals.

Table 3. Effects of different parts of *Tamarindus indica* fruit aqueous extracts on body weight gain in the experimental groups.

Groups	Week 1 (g)	(%) of Change	Week 2 (g)	(%) of Change
Normal Control	209.60 ± 1.91	-	210.64 ± 2.14	1.64 ± 0.87
Hypertensive Control	244.61 ± 3.24^{a***}	16.72 ± 2.48	265.15 ± 3.58^{a***}	26.51 ± 1.92
Reference Control	221.69 ± 2.82^{b***}	5.78 ± 1.58	228.15 ± 2.76^{b***}	8.86 ± 1.48
FRiST 50	229.63 ± 1.93^{b***}	9.56 ± 1.20	232.96 ± 2.60^{b***}	11.15 ± 1.57
SRiST 50	236.54 ± 1.12^{b*}	12.86 ± 0.63	248.43 ± 2.59^{b***}	18.53 ± 0.54
FRaST 50	241.12 ± 2.34	15.05 ± 1.92	246.93 ± 2.18^{b**}	17.83 ± 1.91
FSwT 50	234.74 ± 1.62^{b*}	12.00 ± 0.46	243.13 ± 2.16^{b***}	16.00 ± 0.48
FRiST 100	230.61 ± 4.94^{b*}	10.04 ± 2.78	238.94 ± 4.77^{b***}	14.00 ± 2.26
SRiST 100	237.57 ± 2.07^{b*}	13.35 ± 1.18	251.63 ± 3.92^{b**}	20.05 ± 1.38
FRaST 100	243.08 ± 2.19^{b*}	15.99 ± 1.88	256.33 ± 3.40^{b*}	22.31 ± 2.52
FSwT 100	235.68 ± 3.48^{b*}	12.45 ± 1.55	246.13 ± 2.50^{b***}	17.43 ± 0.92

Each value represents a mean ± SD for n = 5 and was analyzed by one-way ANOVA followed by t-tests; FRiST 50 & FRiST 100 = Flesh of Ripen Sour Tamarind aqueous extract at 50 g/kg BW and 100 mg/kg BW; SRiST 50 & SRiST 100 = Seed of Ripen Sour Tamarind aqueous extract at 50 g/kg BW and 100 mg/kg BW; FRaST 50 & FRaST 100 = Flesh of Raw Sour Tamarind aqueous extract at 50 mg/kg BW and 100 mg/kg BW; FSwT 50 & FSwT 100= Flesh of Sweet Tamarind aqueous extract at 50 mg/kg BW and 100 mg/kg BW. Normal control vs. hypertensive control: $p < 0.05 = a^{*}$; $p < 0.001 = a^{***}$; Hypertensive control vs. treatment controls: $p < 0.05 = b^{*}$; $p < 0.01 = b^{**}$; $p < 0.001 = b^{***}$.

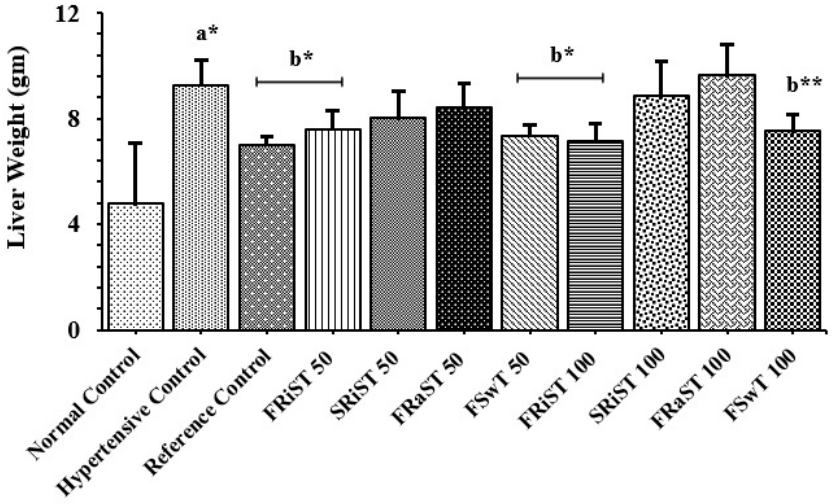

Preprints (www.preprints.org) | NOT PEER-REVIEWED | Posted: 12 June 2023 doi:10.20944/preprints202306.0819.v1

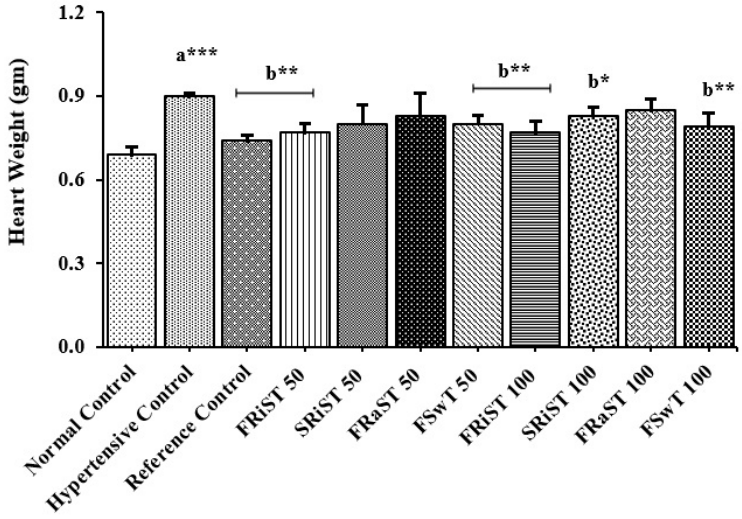

Figure 1. Effects of tamarind products on liver weight (a) and heart weight (b). Each bar represented a mean ± SD for n = 5 and was analyzed by one-way ANOVA followed by t-tests; FRiST 50 & FRiST 100 = Flesh of Ripen Sour Tamarind aqueous extract at 50 mg/kg BW and 100 mg/kg BW; SRiST 50 & SRiST 100 = Seed of Ripen Sour Tamarind aqueous extract at 50 mg/kg BW and 100 mg/kg BW; FRaST 50 & FRaST 100 = Flesh of Raw Sour Tamarind aqueous extract at 50 mg/kg BW and 100 mg/kg BW; FSwT 50 & FSwT 100= Flesh of Sweet Tamarind aqueous extract at 50 mg/kg BW and 100 mg/kg BW. Normal control vs. hypertensive control: $p < 0.05 = a^{*}$; $p < 0.001 = a^{***}$; Hypertensive control vs. treatment controls: $p < 0.05 = b^{*}$; $p < 0.01 = b^{**}$; $p < 0.001 = b^{***}$.

3.4. Effects of Tamarind products on biochemical parameters

3.4.1. Effect of the extracts on serum lipid profile

The effects of tamarind products on the serum lipid profile including total cholesterol (TC), triglyceride (TG), LDL, VLDL & HDL are summarized in **Table 4**. The flesh of ripen sour tamarind (FRiST50) at 50 mg/kg body was found to maximally reduce the total cholesterol level. All the treatment groups except sweet tamarind (FSwT50) and raw sour tamarind (FRaST100) significantly ($P < 0.05$) minimized the cholesterol levels compared to the normal control group. The flesh of raw sour tamarind (FRaST50) opted to achieve the highest reduction of TG level while SRiST50, FSwT and FSwT were also found to significantly minimize the TG levels compared to positive control. All the treatments significantly ($P < 0.01$) downturned the LDL levels and increased the HDL levels compared to the hypertensive control group. Lower doses of all the treatments displayed the VLDL decrement which is statistically significant compared to the hypertensive group. Interestingly, FSwT100 showed no VLDL-reducing effect.

Table 4. Effects of Tamarind products on serum lipid profiles of experimental groups.

Groups	Cholesterol (mg/dL)	Triglycerides (mg/dL)	LDL (mg/dL)	HDL (mg/dL)	VLDL (mg/dL)
Normal Control	38.17 ± 4.17	51.57 ± 2.59	6.76 ± 0.39	47.14 ± 0.57	14.91 ± 0.76
Hypertensive Control	81.59 ± 5.13^{a***}	86.38 ± 2.49^{a***}	33.56 ± 3.10^{a***}	31.24 ± 0.68^{a**}	21.27 ± 0.61^{a***}
Reference Control	58.19 ± 6.18^{b**}	55.16 ± 2.65^{b***}	15.77 ± 1.55^{b***}	48.42 ± 0.74^{b***}	17.73 ± 0.55^{b***}
FRiST 50	39.64 ± 6.71^{b**}	75.87 ± 1.56^{b**}	8.22 ± 0.36^{b***}	50.48 ± 0.80^{b***}	13.92 ± 0.56^{b***}
FRiST 100	46.12 ± 5.30^{b***}	73.35 ± 3.27^{b***}	10.53 ± 1.14^{b***}	51.28 ± 0.68^{b***}	18.63 ± 1.45^{b*}
SRiST 50	45.58 ± 5.72^{b**}	62.11 ± 2.97^{b***}	8.68 ± 0.30^{b***}	46.60 ± 0.72^{b***}	11.34 ± 0.71^{b***}

Preprints (www.preprints.org) | NOT PEER-REVIEWED | Posted: 12 June 2023 doi:10.20944/preprints202306.0819.v1

SRiST 100	41.23 ± 4.17b***	62.19 ± 5.75b**	9.22 ± 0.71b***	50.42 ± 0.88b***	10.73 ± 0.53b***
FRaST 50	52.43 ± 9.60^{b**}	58.84 ± 3.71^{b***}	9.01 ± 0.41^{b***}	44.33 ± 0.80^{b***}	10.79 ± 0.89^{b***}
FRaST 100	65.51 ± 6.22^{b***}	95.48 ± 15.30	10.72 ± 1.52^{b***}	51.50 ± 0.94^{b***}	21.44 ± 2.47
FSwT 50	68.34 ± 3.28^{b*}	62.28 ± 4.64^{b***}	11.89 ± 1.27^{b***}	49.27 ± 2.16^{b***}	12.37 ± 0.93^{b***}
FSwT 100	42.83 ± 9.40^{b**}	59.75 ± 4.53^{b***}	6.43 ± 0.46^{b***}	52.47 ± 2.24^{b***}	15.37 ± 0.70^{b***}

Each value represented a mean ± SD for n = 5 and was analyzed by one-way ANOVA followed by t-tests; FRiST 50 & FRiST 100 = Flesh of Ripen Sour Tamarind aqueous extract at 50 mg/kg BW and 100 mg/kg BW; SRiST 50 & SRiST 100 = Seed of Ripen Sour Tamarind aqueous extract at 50 mg/kg BW and 100 mg/kg BW; FRaST 50 & FRaST 100 = Flesh of Raw Sour Tamarind aqueous extract at 50 mg/kg BW and 100 mg/kg BW; FSwT 50 & FSwT 100= Flesh of Sweet Tamarind aqueous extract at 50 mg/kg BW and 100 mg/kg BW. Normal control vs. hypertensive control: $p < 0.05 = a^{*}$; $p < 0.001 = a^{***}$; Hypertensive control vs. treatment controls: $p < 0.05 = b^{*}$; $p < 0.01 = b^{**}$; $p < 0.001 = b^{***}$.

3.4.2. Effect of the extracts on serum enzyme activities

The changes in ALT, AST, and ALP levels at the end of the intervention are presented in Table **5**. The serum ALT level was found to be maximally attenuated by the FRiST50 and FSwT100 while other treatments also showed a significant reduction of ALT levels. The FRiST50 and FSwT100 treatments, among all other groups, showed the highest decrement of AST levels while the values were statistically significant (P< 0.05) compared to both the hypertensive group and positive control (PC) group. Excitingly, the SRiST50 was found to show the maximum and significant decrease of ALP levels; while it was very consistent in reducing the ALT, AST, and ALP levels. #

Table 5. Effects of tamarind products on serum enzymes of experimental groups.

Groups	ALT (IU/L)	AST (IU/L)	ALP (IU/L)
Normal Control	56.26 + 1.73	48.29 + 8.35	361.33 + 4.36
Hypertensive Control	297.59 + 12.06^{a***}	166.77 + 5.78^{a***}	582.93 + 8.06^{a***}
Reference Control	128.94 + 4.65^{b***}	60.06 + 3.24^{b***}	466.73 + 4.13^{b***}
FRiST50	120.44 + 5.01^{b***}	54.98 + 3.44^{b***}	451.53 + 6.31^{b***}
FRiST100	187.84 + 4.46^{b***}	98.97 + 3.37^{b***}	291.85 + 5.33^{b***}
SRiST50	129.22 + 5.94^{b***}	64.58 + 3.94^{b***}	222.83 + 5.18^{b***}
SRiST100	147.86 + 3.20^{b***}	70.01 + 3.03^{b***}	273.86 + 4.13^{b***}
FRaST50	145.14 + 4.32^{b***}	69.26 + 2.84^{b***}	385.07 + 5.45^{b***}
FRaST100	133.00 + 2.42^{b***}	73.44 + 3.67^{b***}	382.18 + 6.18^{b***}
FSwT50	161.73 + 5.56^{b***}	58.02 + 0.82^{b***}	365.65 + 7.19^{b***}
FSwT100	99.88 + 3.15^{b***}	62.57 + 1.95^{b***}	310.88 + 12.81^{b***}

Each value represented a mean ± SD for n = 5 and was analyzed by one-way ANOVA followed by t-tests; FRiST 50 & FRiST 100 = Flesh of Ripen Sour Tamarind aqueous extract at 50 mg/kg BW and 100 mg /kg BW; SRiST 50 & SRiST 100 = Seed of Ripen Sour Tamarind aqueous extract at 50 mg/kg BW and 100 mg/kg BW; FRaST 50 & FRaST 100 = Flesh of Raw Sour Tamarind aqueous extract at 50 mg/kg BW and 100 mg/kg BW; FSwT 50 & FSwT 100= Flesh of Sweet Tamarind aqueous extract at 50 mg/kg BW and 100 mg/kg BW. Normal control vs. hypertensive control: $p < 0.05 = a^{*}$; $p < 0.001 = a^{***}$; Hypertensive control vs. treatment controls: $p < 0.05 = b^{*}$; $p < 0.01 = b^{**}$; $p < 0.001 = b^{***}$.

3.4.3. Effects of the extracts on the CRP, troponin I (cTnI), and liver glycogen levels

The effect of tamarind products on the CRP, troponin I and liver glycogen level is summarized in Figure 2. The C-reactive protein of all the groups except the NC group is observed to be increased due to the cholesterol induction. The cholesterol-induced increase of CRP levels was discovered to be significantly minimized by the treatments of FRiST50, FRaST50, SRiST50, FSwT100, and SRiST100 groups. Another very crucial biomarker, serum troponin I level was noticed to be decreased in the treatment groups. The sweet tamarind at the dose of 50 mg/kg bw (FSwT50) was found to be the most effective to decrease the troponin I level among the treatments, although all the treatments significantly reduced Troponin I except the SRiST100 which has no effect. Liver glycogen has been

Preprints (www.preprints.org) | NOT PEER-REVIEWED | Posted: 12 June 2023 doi:10.20944/preprints202306.0819.v1

impacted by almost all the doses while the flesh of raw sour tamarind at the dose of 50 mg/kg/bd (FRaST50) was found to maximally and significantly potentiate the liver glycogen compared to the reference control. At a glance, the sweet tamarind especially SRiST100 was better to increase the animal liver glycogen than the other forms and doses of tamarinds.

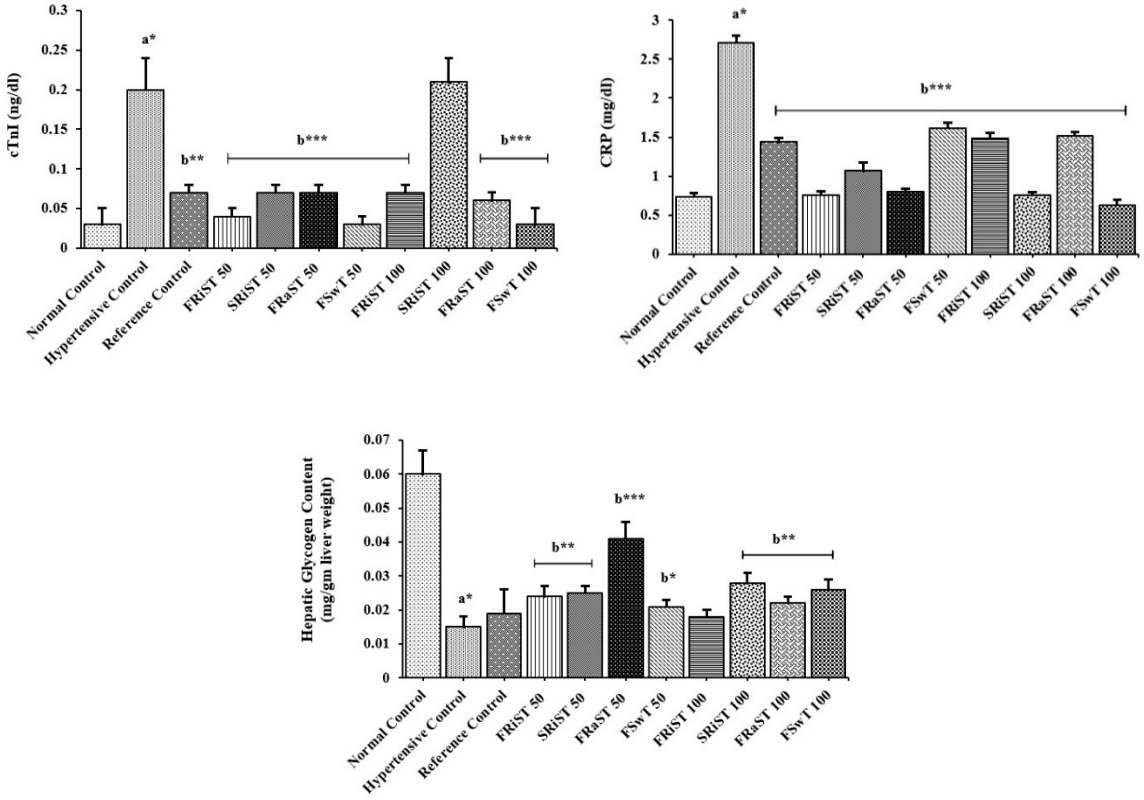

Figure 2. Effects of tamarind products on CRP (a), cTnI (b), and hepatic glycogen content (c). Each bar represented a mean ± SD for n = 5 and was analyzed by one-way ANOVA followed by t-tests; FRiST 50 & FRiST 100 = Flesh of Ripen Sour Tamarind aqueous extract at 50 mg/kg BW and 100 mg/kg BW; SRiST 50 & SRiST 100 = Seed of Ripen Sour Tamarind aqueous extract at 50 mg/kg BW and 100 mg/kg BW; FRaST 50 & FRaST 100 = Flesh of Raw Sour Tamarind aqueous extract at 50 mg/kg BW and 100 mg/kg BW; FSwT 50 & FSwT 100= Flesh of Sweet Tamarind aqueous extract at 50 mg/kg BW and 100 mg/kg BW; CRP = C Reactive Protein; cTnI = Cardiac Troponin I. Normal control vs. hypertensive control: $p < 0.05 = a^{*}$; $p < 0.001 = a^{***}$; Hypertensive control vs. treatment controls: $p < 0.05 = b^{*}$; $p < 0.01 = b^{**}$; $p < 0.001 = b^{***}$.

3.5. Effect of tamarind products on heart tissue architecture of cholesterol-induced rat

The impact of light microscopic examination of the cardiac muscle of the control group showed **(Figure 3)** a normal myofibrillar structure with striations, branched appearance, anastomosing cardiac myocytes with Central nuclei, acidophilic sarcoplasm, adjacent myofibrils, and prominent intercalated disc. Photomicrographs of some sections in the cardiac muscle from treated group FRiST50, FSwT50, FRaST50, SRiST50, FRaST100, and FSwT100 showed well-maintained separation of muscle fibers and peripheral nuclei in some fiber's nuclei. disarrangement of cardiac myocyte, cytoplasmic vacuolation, degeneration of muscle fibers, and vascular infiltration observed in the slide of group FRiST100 and SRiST 100.

 doi:10.20944/preprints202306.0819.v1

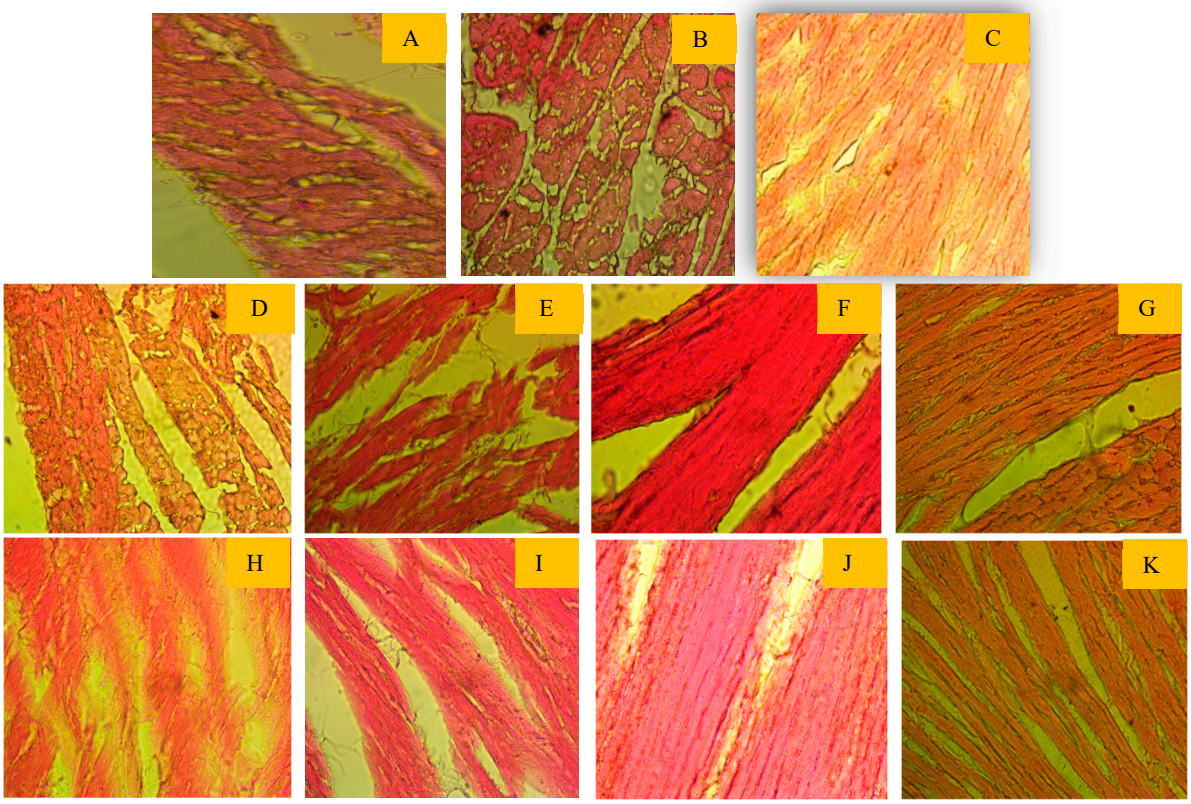

Figure 3. Histopathological image (magnification 10 × 40) of heart tissue of the experimental animals from the groups: A. Normal control, B. Hypertensive control, C. Atenolol control (positive control), D. FRiST50, E. SRiST50, F. FRaST50, G. FSwT50, H. FRiST100, I. SRiST100, J. FRaST100, and K. FSwT100.

3.6. Phytochemical contents of the tamarind extracts

The GC-MS spectra of the sour tamarind and sweet tamarind extracts are shown in **Figure 4.** The array of compounds is presented in Table **6**. Cyclohexanamine, 2-Furanethanol, beta. -methoxy-(S)-;N-3-butenyl-N-methyl;1-Ethyl-2-hydroxymethylimida Hydrazinecarboxamide, 2-(2-methylcyclohexylidene)- zol, Fumaric acid, butyl 3-methylbut-3-enyl ester, 5-(Hydroxymethyl)-2-(dimethoxy methyl) fural, 3-O-Methyl-d-glucose are noted as the constituents displaying the highest occurrence. Moreover, data showed the presence in small amounts of N-Glycylglycine, hexadecenoic acid, 1,1- dimethyl ethyl ester, 4H-Pyran-4-one, 2,3-dihydro-3,5- dihydroxy-6-methyl-, cis-13-Octadecenoic acid, 5-(Hydroxymethyl)-2- (dimethoxymethyl)furan.

Preprints (www.preprints.org) | NOT PEER-REVIEWED | Posted: 12 June 2023 doi:10.20944/preprints202306.0819.v1

Table 6. Gas chromatography-mass spectrometry analysis data for fresh and ripen tamarind.

		Sour Tamarind Flesh
RT	Abd	Compounds
3.558	0.22	Dodecanoic acid, 3-hydroxy-
3.631	0.36	N-Glycylglycine
3.763	0.87	2,5,5-Trimethyl-3-hexyn-2-ol
3.850	0.26	3-Furancarboxylic acid
4.001	1.46	Cyclohexanamine, N-3-butenyl-N-methyl-
4.087	1.91	Methyl 2-furoate
4.208	0.47	2-Butenedioic acid (E)-, monomethyl ester
4.317	0.21	Hexadecanoic acid, 1,1-dimethylethyl ester
4.393	0.40	Levoglucosenone
4.477	0.59	Heptane, 4-ethyl-
4.635	0.49	Glutaric acid, 3-heptyl propyl ester
4.748	2.10	H-Pyran-4-one, 2,3-dihydro-3,5-dihydroxy-6
4.783	2.31	1-(2-Thienyl)-1-propanone
4.983	0.01	2-Furanethanol, .beta.-methoxy-(S)-
5.058	0.03	2(3H)-Furanone, dihydro-4-hydroxy-
5.167	0.06	4H-Pyran-4-one, 3,5-dihydroxy-2-methyl-
5.225	0.40	1,3-Propanediol, 2-(hydroxymethyl)-2-nitro-
5.284	0.24	2-Propyl-1-pentanol
5.773	15.22	1-Ethyl-2-hydroxymethyl imidazole
5.796	1.80	Fumaric acid, butyl 3-methylbut-3-enyl ester
6.005	0.58	7-Dimethyl(prop-2-enyl)silyloxytridecane
6.208	0.21	cis-13-Octadecenoic acid
6.325	2.26	5-(Hydroxymethyl)-2-(dimethoxymethyl)furan
6.449	1.30	Decanoic acid, 3-methyl-
6.640	0.86	2,4-Dimethyl-3-pentanol acetate
6.811	0.54	Silane, dimethyldi(but-3-enyloxy)-
7.213	0.22	.alpha.-Methyl mannofuranoside
7.538	2.36	Glutamine
7.636	0.43	3-Chloro-6-methoxy-2-methyl benzoic acid, m
7.825	0.13	Carbonic acid, butyl ethyl ester
7.958	0.07	(S)-(-)-1,2,4-Butanetriol, 4-acetate
8.036	0.19	1-Methyl-1-n-pentyloxy-1-silacyclobutane
8.367	0.25	D-Mannoheptulose
8.642	0.10	2-t-Butyl-4-oxo oxazolidine-3-carboxylic acid
9.150	5.40	D-Allose
9.281	3.89	.beta.-D-Glucopyranose, 1,6-anhydro-
9.779	0.20	1,2-O-Isopropylidene-D-xylofuranose, TBDM
10.147	0.42	Acetic acid, 2-ethylbutyl ester
10.317	0.13	3-Methylmannoside
10.400	0.32	4-Hydroxy-3-[3-(2-hydroxy-5-methoxy-phenyl
10.863	3.97	1,6-Anhydro-.beta.-D-glucofuranose
11.226	0.50	Hydrazinecarboxamide, 2-(2-methylcyclohexy
12.565	37.25	3-O-Methyl-d-glucose
13.908	0.30	1-(2-Fluorophenyl)pyrazole-4-carboxylic acid
14.908	0.49	4-Hydroxy-2-hydroxymethyl-6-methylpyrimidi
17.958	0.29	R-(+)-Methyl-3-isopropyl-6-oxoheptanoate
18.690	0.32	E-8-Methyl-7-dodecane-1-ol acetate

		SweetTamarind flesh
RT	Abd	Compounds
3.573	0.29	n-PROPYL NONYL ETHER
3.646	0.39	dl-2-Aminocaprylic acid
3.733	0.29	Pentanoic acid, 5-(1-oxo-2-phenylethylamino)
3.793	0.54	2,5-Dimethylfuran-3,4(2H,5H)-dione
4.025	1.96	Thymine
4.094	0.58	Furyl hydroxymethyl ketone
4.482	0.31	Aluminum, triethyl-
4.643	0.28	Ethanamine, N-ethyl-N-nitroso-
4.766	2.30	4H-Pyran-4-one, 2,3-dihydro-3,5-dihydroxy-6
4.892	0.32	N,N-Dimethyl-O-(1-methyl-butyl)-hydroxylam
4.942	0.17	2(3H)-Furanone, dihydro-4-hydroxy-
5.173	0.56	1,3,2-Dioxaborolan-4-one, 2-ethyl-5-methyl-
5.333	0.57	Pentanoic acid, 2-isopropoxyphenyl ester
5.457	0.16	Piperidine, 1-nitroso-
5.722	12.74	1-Ethyl-2-hydroxymethylimidazole
5.911	0.31	4-(Prop-2-enoyloxy)pentadecane
6.292	0.27	Cyclobutanecarboxylic acid, heptyl ester
6.389	0.50	2-Methyl-1-di(tert-butyl)silyloxypropane
6.595	0.59	3-cis-Methoxy-5-cis-methyl-1R-cyclohexanol
6.776	0.48	2,4-Dimethyl-3-pentanol acetate
7.202	0.38	Pentane, 2,2,4,4-tetramethyl-3-methoxy-
7.449	2.12	7-Tridecanol
7.567	3.07	Succinic acid, di(but-2-en-1-yl) ester
7.791	0.55	Benzene, 1-chloro-4-methoxy-
8.038	0.27	Galactopyranoside, 1-octylthio-1-deoxy-
8.233	0.18	2-Acetyl-5-methylthiophene
8.362	1.05	Sucrose
8.558	0.18	Dinocap
9.225	0.25	1,6-Anhydro-.beta.-d-talopyranose
9.390	2.77	1,3-Propanediol, 2-(hydroxymethyl)-2-nitro-
10.618	0.28	.alpha.-Methyl-l-sorboside
10.753	1.34	1,6-Anhydro-.beta.-D-glucofuranose
10.043	0.44	.alpha.-Methyl mannofuranoside
12.408	16.53	D-Fructose, 3-O-methyl-
12.959	44.16	3-O-Methyl-d-glucose
27.663	0.98	0.98.gamma.-Sitosterol

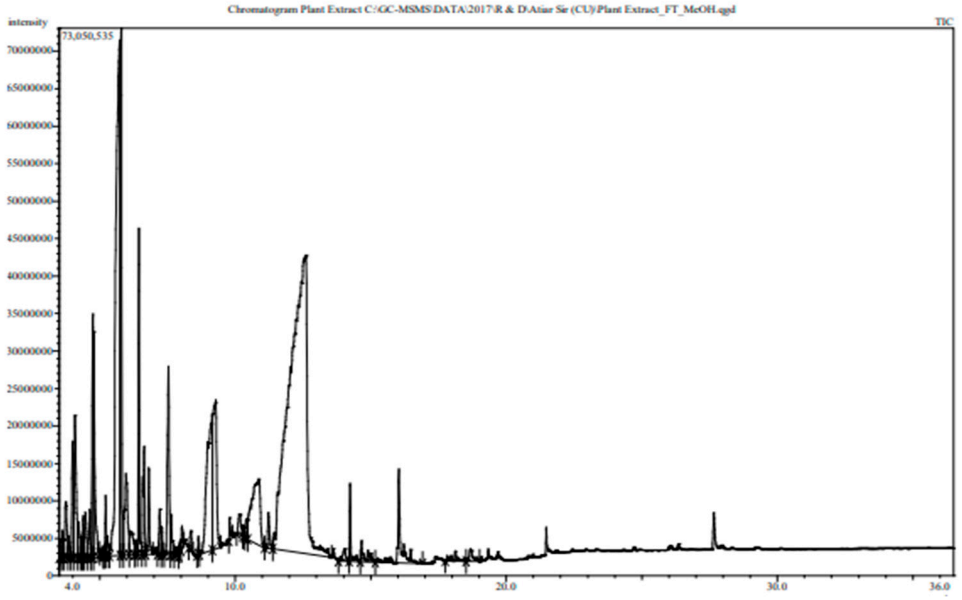

Preprints (www.preprints.org) | NOT PEER-REVIEWED | Posted: 12 June 2023 doi:10.20944/preprints202306.0819.v1

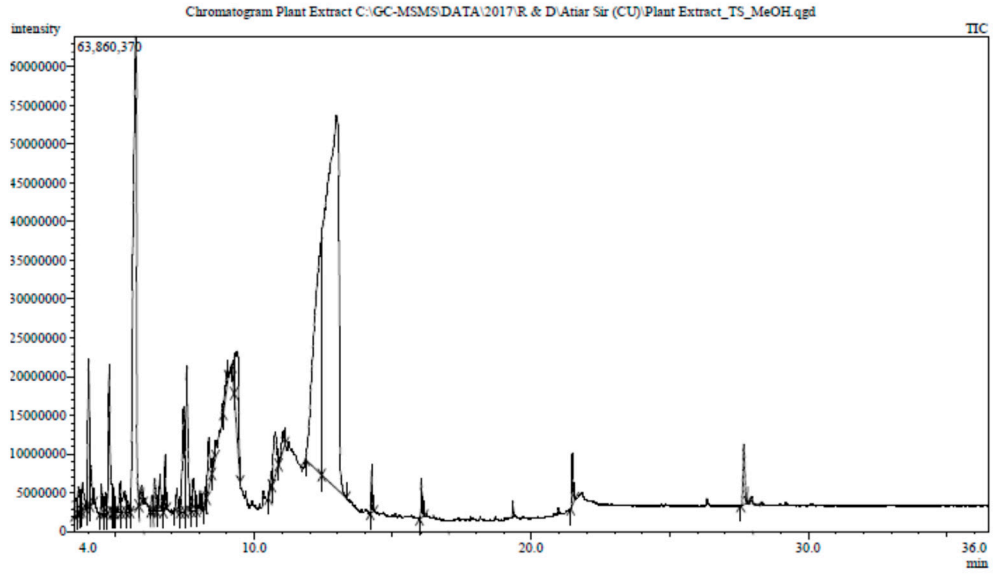

Figure 4. Gas chromatography-mass spectrometry profile of aqueous extract of *Tamarindus indica*; (a) flesh, ripen sour, and (b) flesh, ripen sweet; was obtained from GC-MS with electron impact ionization (EI) method on a gas chromatograph (GC17A, Shimadzu Corporation, Kyoto, Japan) coupled to a mass spectrometer (GC-MS TQ 8040, Shimadzu Corporation, Kyoto, Japan). The inlet temperature was set at 260 °C, and the oven temperature was programmed as 70 °C (0 min); 10 °C, 150 °C (5 min); 12 °C, 200 °C (15 min); 12 °C, 220 °C (5 min).

3.7. Impacts of ligand-receptor interactions in In silico Molecular docking analysis

Docking analysis of antihypertensive activity through pharmacokinetic properties is shown in **Table 8.** This study showed that eight major receptors Tyrosine Hydroxylase (PDB ID: 1TOH), BETA-1 subunit of the soluble guanylyl cyclase (PDB ID: 3HLS), Human High-conductance Ca^{2+} gated K^{+} Channel (BK Channel)(PDB ID: 3NAF), Nuclear hormone receptor PPAR-gamma(PDB ID: 3R8A), Human Angiotensin Receptor (PDB ID: 4YAY), Macrocyclic IL-17A antagonists (PDB ID: 5HI3), Human soluble guanylate cyclase(PDB ID: 6JT0) was involved to explore anti-hypertensive activity. In the case of the Tyrosine Hydroxylase (PDB ID: 1TOH), BETA-1 subunit of the soluble guanylyl cyclase (PDB ID: 3HLS), nuclear hormone receptor PPAR-gamma (PDB ID: 3R8A), gamma-sitosterol showed the docking score -7.6 (**Figure 5**). The docking score was -7.7 for the interaction of gamma-sitosterol with Human High-conductance Ca^{2+} gated K^{+} Channel (BK Channel) (PDB ID: 3NAF). The interaction of the same compound with Human Angiotensin Receptor (PDB ID: 4YAY), Macrocyclic IL-17A antagonists (PDB ID: 5HI3), Human soluble guanylate cyclase (PDB ID: 6JT0) had the docking score -9.3, -9.1, -7 respectively (**Table 9**). The best binding affinity score of gamma-sitosterol was found with guanylate cyclase (PDB ID: 6JT0) which is -9.3.

Preprints (www.preprints.org) | NOT PEER-REVIEWED | Posted: 12 June 2023 doi:10.20944/preprints202306.0819.v1

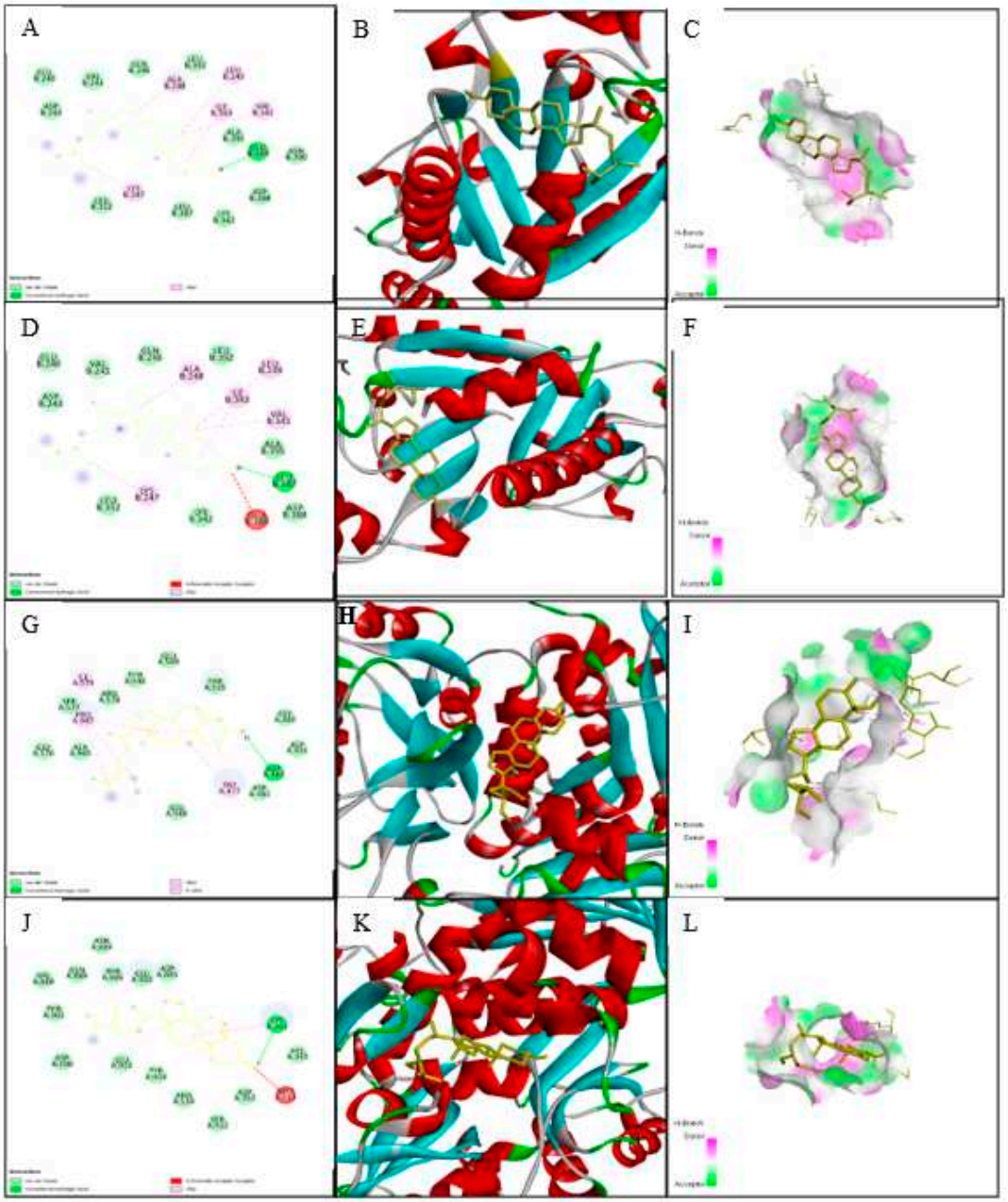

Preprints (www.preprints.org) | NOT PEER-REVIEWED | Posted: 12 June 2023 doi:10.20944/preprints202306.0819.v1

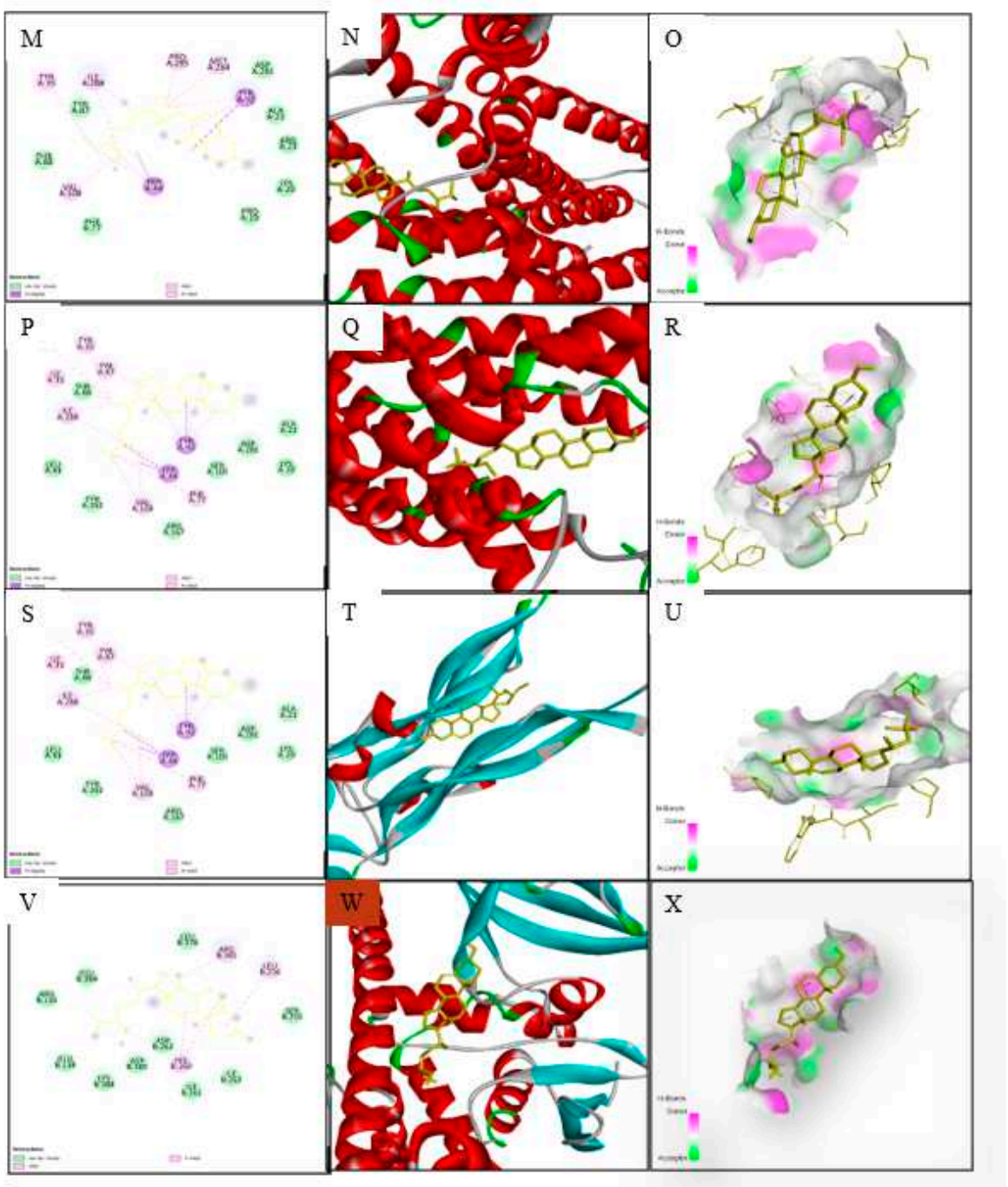

Figure 5. Docking analysis of (A,B,C) 2D , 3D and ligand-receptor interaction view of Gamma-sitosterol:Best binding affinity with Tyrosine Hydroxylase; (D,E,F)2D , 3D and ligand-receptor interaction view of Gamma-sitosterol:Best binding affinity with BETA-1 subunit of the soluble guanylyl cyclase (G,H,I)2D , 3D and ligand-receptor interaction view of Gamma-sitosterol:Best binding affinity with Human High-conductance Ca2+ gated K+ Channel (BK Channel); (J,K,L) 2D , 3D and ligand-receptor interaction view of Gamma-sitosterol:Best binding affinity with Nuclear hormone receptor PPAR-gamma receptor;(M,N,O) 2D , 3D and ligand-receptor interaction view of Gamma-sitosterol: Best binding affinity with Human Angiotensin Receptor;(P,Q,R) 2D , 3D and ligand-receptor interaction view of Gamma-sitosterol: Best binding affinity with Thermolysin; (S,T,U) 2D , 3D and ligand-receptor interaction view of Gamma-sitosterol: Best binding affinity with Macrocyclic IL-17A antagonists and (V,W,X) 2D , 3D and ligand-receptor interaction view of Gamma-sitosterol: Best binding affinity with Human soluble guanylate cyclase.

Preprints (www.preprints.org) | NOT PEER-REVIEWED | Posted: 12 June 2023 doi:10.20944/preprints202306.0819.v1

3.7.1. Impacts on pharmacokinetic and toxicological properties

The pharmacokinetic properties of different compounds are investigated using QikProp, SwissADME/T (absorption, distribution, metabolism, and excretion/transport) prediction tool. From this study, (1-Ethyl-1H-imidazol-2-yl) methanol, 4H-Pyran-4-one,2-Furanmethanol,5-(dimethoxymethyl)-,7-Tridecanol, Glutamine, 1-(2-Thienyl)-propanone, Succinic acid, di(but-2-en-1-yl) ester,2-(Hydroxymethyl)-2-nitro-1,3-propanediol did not disobey the Lipinski's and rule Veber's rule. Hence, these nine compounds exhibited drug-like attributes (Table 7) and were more likely to be orally available as they maximally obeyed Lipinski's rule and Veber's rule. On the other hand, D-Mannoheptulose and Gamma-sitosterol both have one violation. Furthermore, toxicological properties were also predicted using the admetSAR online server, where the study demonstrated that compounds are non-carcinogenic except 7-Tridecanol (Table 8). As a result, ten bioactive ingredients could be investigated for prospective therapeutic candidates with strong oral bioavailability through additional thorough studies, such as an animal model clinical trial.

Table 7. Pharmacokinetic properties of the selected compounds in different *T. indica* extract.

Tamarind Compounds	Lipinski Rules				Lipinski's Violations (≤ 1)	Veber Rules	
	MW (< 500)	HBA (< 10)	HBD (< 5)	Log P (≤ 5)		Nrb (≤ 10)	TPSA (≤ 140 Å²)
(1-Ethyl-1H-imidazol-2-yl)methanol	126.16	2	1	0.21	0	2	38.05
4H-Pyran-4-one	144.13	4	2	-0.22	0	0	66.76
2-Furanmethanol,5-(dimethoxymethyl)-	172.18	4	1	0.60	0	4	51.83
7-Tridecanol	200.36	1	1	4.28	0	10	20.23
D-Mannoheptulose	210.18	7	6	-2.65	1	7	107.22
Gamma-sitosterol	414.71	1	1	7.19	1	6	20.23
Glutamine	146.14	4	3	-1.81	0	4	106.41
1-(2-Thienyl)-1-propanone	140.20	1	0	2.03	0	2	45.31
Succinic acid, di(but-2-en-1-yl) ester	226.27	4	0	2.26	0	9	52.60
2-(Hydroxymethyl)-2-nitro-1,3-propanediol	151.12	5	3	-1.84	0	4	106.51

MW, molecular weight; HBA, hydrogen bond acceptor; HBD, hydrogen bond donor, Log P, liphophilicity.

Table 8. Toxicological properties of the selected compounds in *Tamarindus indica*.

Compounds	Parameters			
	Ames toxicity	Carcinogens	Acute oral toxicity	Rat Acute Toxicity
(1-Ethyl-1H-imidazole-2-yl)methanol	NAT	NC	III	2.2439
4H-Pyran-4-one	AT	NC	III	1.7885
2-Furanmethanol,5-(dimethoxymethyl)-	NAT	NC	III	2.0967
7-Tridecanol	NAT	C	III	1.7615
D-Mannoheptulose	NAT	NC	IV	1.4430
Gamma-sitosterol	NAT	NC	I	2.6561
Glutamine	NAT	NC	IV	1.2587
1-(2-Thienyl)-1-propanone	NAT	NC	III	2.1210
Succinic acid, di(but-2-en-1-yl) ester	NAT	NC	III	1.8106
2-(Hydroxymethyl)-2-nitro-1,3-propanediol	NAT	NC	III	2.0756

NAT, Non Ames toxic; AT, Ames toxic; C, Carcinogenic; NC, Non-carcinogenic; Category-I (≤50 mg/kg); Category-III (50 mg/kg < LD50 < 300 mg/kg); Category-IV (300 mg/kg < LD50 < 2000 mg/kg).

Preprints (www.preprints.org) | NOT PEER-REVIEWED | Posted: 12 June 2023 doi:10.20944/preprints202306.0819.v1

Table 9. The binding affinity of most bioactive compounds (Gamma-sitosterol) with different proteins.

	Binding Affinity
Protein Name	Gamma-sitosterol (Compound ID:457801)
Tyrosine Hydroxylase (PDB ID: 1TOH)	-7.6
BETA-1 subunit of the soluble guanylyl cyclase(PDB ID: 3HLS)	-7.6
Human High-conductance Ca2+ gated K+ Channel (BK Channel)(PDB ID: 3NAF)	-7.7
Nuclear hormone receptor PPAR-gamma (PDB ID: 3R8A)	-7.6
Human Angiotensin Receptor (PDB ID: 4YAY)	-9.3
Thermolysin (PDB ID: 5DPF)	-9.6
Macrocyclic IL-17A antagonists (PDB ID: 5HI3)	-9.1
Human soluble guanylate cyclase (PDB ID: 6JT0)	-7

None of the selected compounds, only 7-Tridecanol was found to show carcinogenicity. 7-Tridecanol is carcinogenic to aquatic organisms, but insufficient data are available on the effect of this substance on human health. Their oral toxicity level was III defying that their LD50 is between 50 mg/kg < LD50 < 300 mg/kg except for D-Mannoheptulose and Glutamine which had an LD50 between 300 mg/kg < LD50 < 2000 mg/kg.

3.7.2. Impacts on drug candidates filtering

The drug-like characteristics of observed small molecules were used to screen the main bioactive components in FRiST and FSwT. These requirements included a molecular weight restriction of 500, a requirement for a minimum of 5 H-bond donors, a requirement for a maximum of 10 H-bond acceptors, a requirement for a moriguchi octanol-water partition coefficient value of 5 or less, and a requirement for an Abbott Bioavailability Score of 0.1 standard values. Surprisingly, 40 detected molecules met the aforementioned requirements and were designated as major bioactive compounds without violating more than one of the previously listed characteristics from where we have selected the top 10 compounds **(Table 7)**.

3.7.3. Common intersected targets of compounds within GeneCard and SwissTargetPrediction Database

The screened bioactive substances were made to obtain compound-relevant targets from online databases. The PubChem chemical library was used to obtain the SMILES code for each component, which was then inserted into the SwissTargetPrediction database searches. The elimination of duplicate targets revealed the presence of 228 targets with relevant genes for hypertension from the String database and 201 targets from the SwissTargetPrediction database that were connected to 10 compounds. Venn diagram analysis showed that there were 14 common targets between those two datasets (Table S1 and Figure 6A).

Preprints (www.preprints.org) | NOT PEER-REVIEWED | Posted: 12 June 2023 doi:10.20944/preprints202306.0819.v1

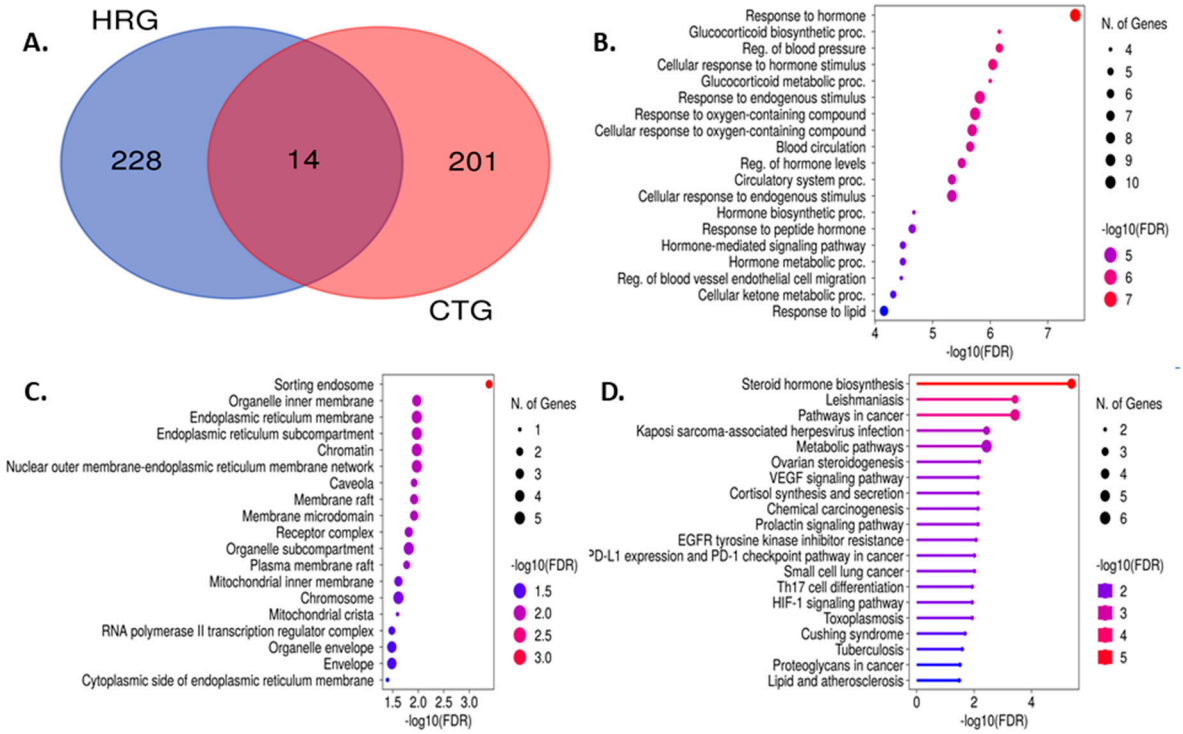

Figure 6. Effect of tamarind on the **A.** Overlapping of genes of hypertension; B, C and D Gene ontology (GO) exploration of compounds.

DisGeNeT, OMIM, and Malacards were used to access three disease-related public databases, resulting in the acquisition of 3081 disease-related targets. The 238 compound-associated targets were then compared to the culled targets to identify the hypertension targets that were directly related to the different FS and TS compounds according to the confidence level above 10 **(Table S2)**. As a result, 14 shared targets that were directly related to hypertension and FRiST and FSwT compounds were identified of which 10 molecules were closely related to typical hypertension targets. The 10 compounds, such as (1-Ethyl-1H-imidazol-2-yl)methanol, 4H-Pyran-4-one, 7-Tridecanol, D-Mannoheptulose, Gamma-sitosterol, Glutamine, 1-(2-Thienyl)-1-propanone, Succinic acid, di(but-2-en-1-yl) ester and 2-(Hydroxymethyl)-2-nitro-1,3-propanediol These substances were produced by the interaction of genes associated with hypertension and target genes for FRiST and FSwT substances.

3.8. Impact on PPI network analysis of 14 common targets

We added those 14 common targets to the STRING database to create a network within them to discover the possible mechanistic insight of FRiST and FSwT to manage hypertension. The STRING method expressed the 14 nodes joined by creating 44 edges at the same time (**Figure 7A**). We then analyzed the network in Cytoscape using a degree value method and cytoHubba applications to examine the crucial main target in the network. The number of degrees for each target was specified as the number of edges connecting to the relevant target nodes. Notably, the best target in the network is identified by a higher degree value. *NR3C1*, *REN*, *PPARG*, and *CYP11B1* were identified as critical targets (36-degree value) in the network for hypertension progression because of this conformity (**Figure 7B**).

Preprints (www.preprints.org) | NOT PEER-REVIEWED | Posted: 12 June 2023 doi:10.20944/preprints202306.0819.v1

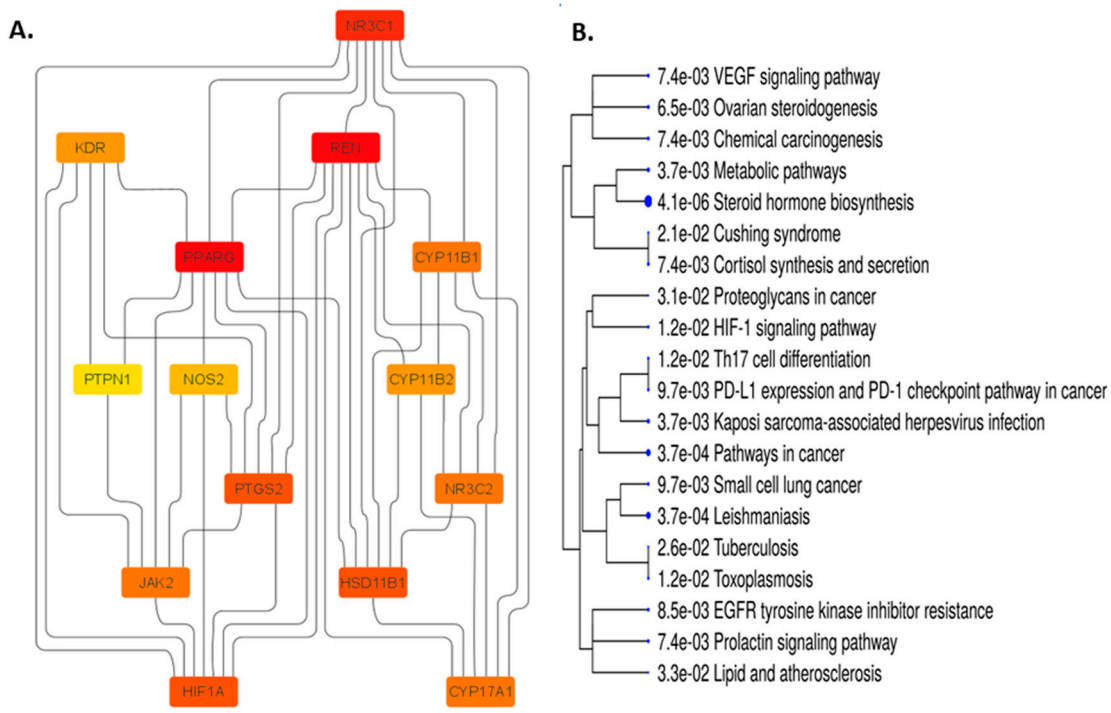

Figure 7. Interactions between proteins (PPI) of common interacting genes utilizing the A. degree algorithm and B. phylogenetic tree of pathways.

3.8.1. Impact on the enrichment analysis of 14 common targets

Through pertinent targets' molecular function (MF), the biological process (BP) in which it participates, and its cellular localization, the GO and KEGG pathway assessment accurately depicts the intersected 14 common targets involved in the hypertension functional process **(Table S3, S4, and S5)**. We examined GO and KEGG pathways using the online application "ShyniGO 0.77". According to the percentage of targets that were enriched in the top 10 MF, BP, and chemical categories, we were able to determine the top 10 MF, BP, and chemical contents for GO **(Figure 6B, 6C, and 6D)**. MF is primarily involved in oxidoreductase activity, acting on paired donors, with incorporation or reduction, Steroid hydroxylase activity, Hsp90 protein binding, Steroid hormone receptor activity, nuclear receptor activity, Ligand-activated transcription factor activity, E-box binding, NADP binding.

3.8.2. Glucocorticoid biosynthetic process

Glucocorticoid metabolic process, Hormone biosynthetic process, Regulation of blood vessels, Endothelial cell migration, Regulation of blood pressure, Hormone-mediated signaling pathway, Hormone metabolic process, Cellular ketone metabolic process, and Blood circulation process were the BPs in which those targets notably participated. However, the aforementioned processes happened in the top 10 CLs, which were sorting endosome, mitochondrial crista, and cytoplasmic side of the endoplasmic reticulum membrane. Caveola, plasma membrane raft, RNA polymerase II transcription regulator complex, membrane raft, Membrane microdomain, Receptor complex. Similar to this, 21 KEGG pathways **(Table S6)** were found at a threshold level of p-value 0.05 in the KEGG pathway enrichment analysis performed using the ShyniGO 0.77 online tool on the 14 possible treatment targets for hypertension in steroid hormones biosynthesis **(Figure 8)**.

Preprints (www.preprints.org) | NOT PEER-REVIEWED | Posted: 12 June 2023 doi:10.20944/preprints202306.0819.v1

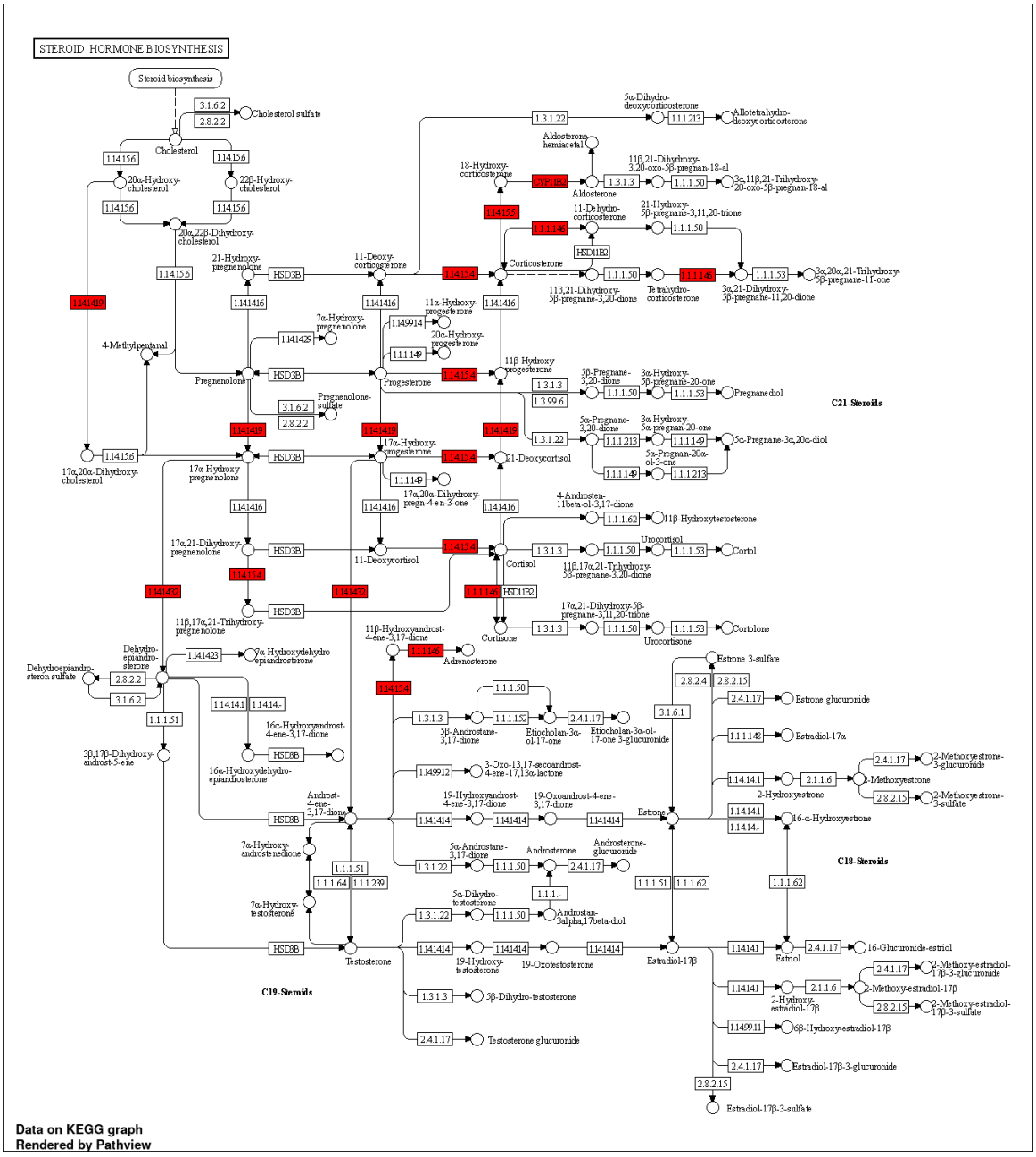

Figure 8. 14 targeted genes showed in red color involved in most significant pathway related to hypertension.

3.9. Molecular dynamics simulations

The dynamic kinematics of the docked complexes were subsequently examined by molecular dynamic simulations at 100 ns using the Desmond module of Schrödinger's suite to study the stability of the protein-ligand combination under *in vivo* mimic conditions. The results were shown in **Figure 9, Figure 10, and Video 1).**

Preprints (www.preprints.org) | NOT PEER-REVIEWED | Posted: 12 June 2023 doi:10.20944/preprints202306.0819.v1

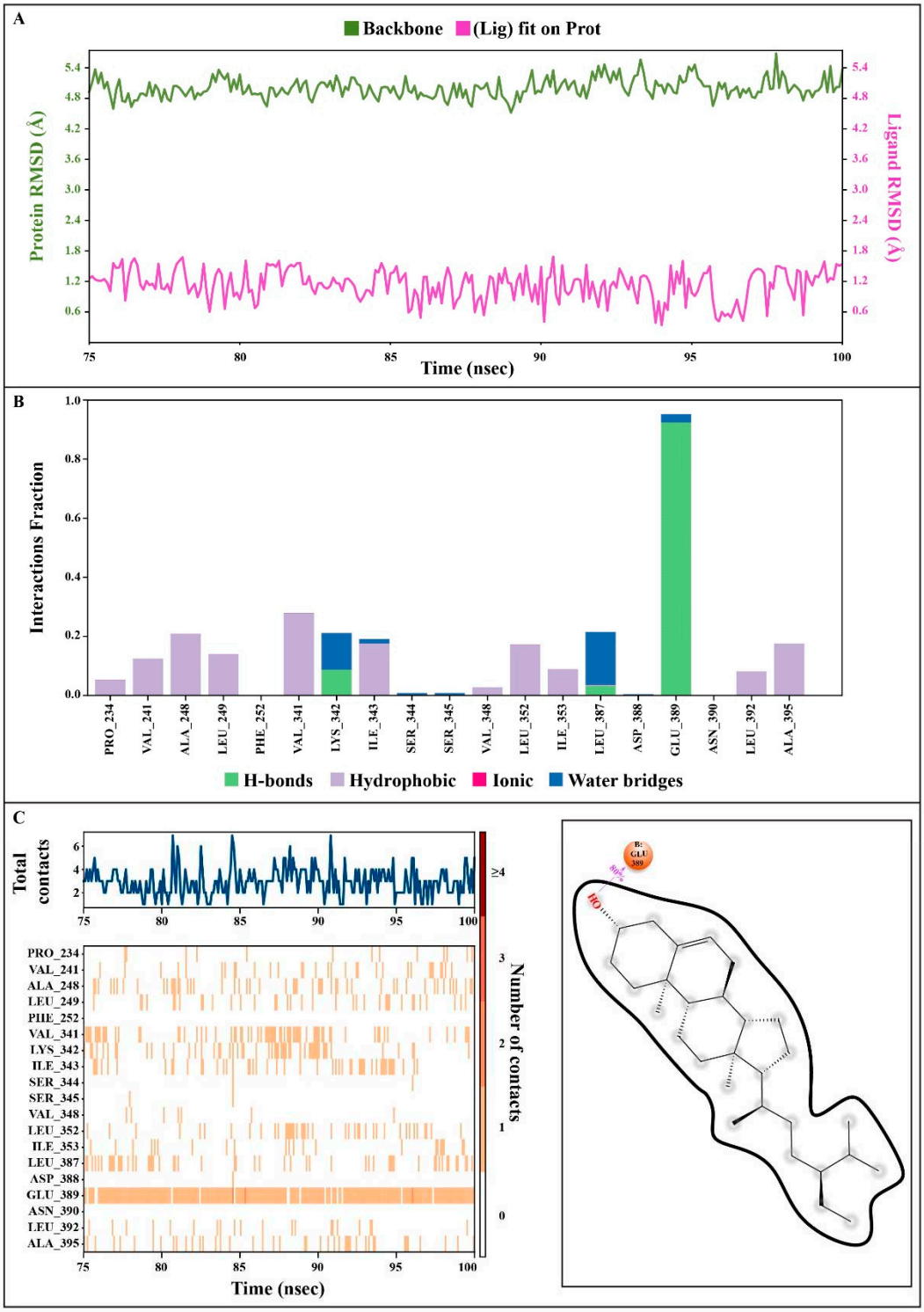

Figure 9. Diagram depicting simulation interactions of a protein-ligand complex under *in vivo* mimic circumstances. (A) Protein-ligand RMSD plot: the left Y-axis represents protein-RMSD, and the right Y-axis represents ligand-RMSD. (B) Histogram of protein-ligand interactions classified as hydrogen bonds (green), hydrophobic (purple), ionic (magenta), and water bridges (blue). (C) A depiction of the interactions and contacts on a timeline: The left top panel depicts the total number of specific

Preprints (www.preprints.org) | NOT PEER-REVIEWED | Posted: 12 June 2023 doi:10.20944/preprints202306.0819.v1

contacts made by the protein with the ligand during the equilibrated trajectory (during the 75.00 to 100.00 ns), whereas the left bottom panel depicts which protein residues interact with the ligand in each trajectory frame. According to the scale to the right of the plot, certain residues make more than one particular contact with the ligand, which is indicated by a deeper shade of orange. The right panel depicts a schematic of precise ligand atom interactions with the protein residues. Interactions that occur more than 30.0% of the time in the chosen trajectory (75.00 to 100.00 ns) are displayed.

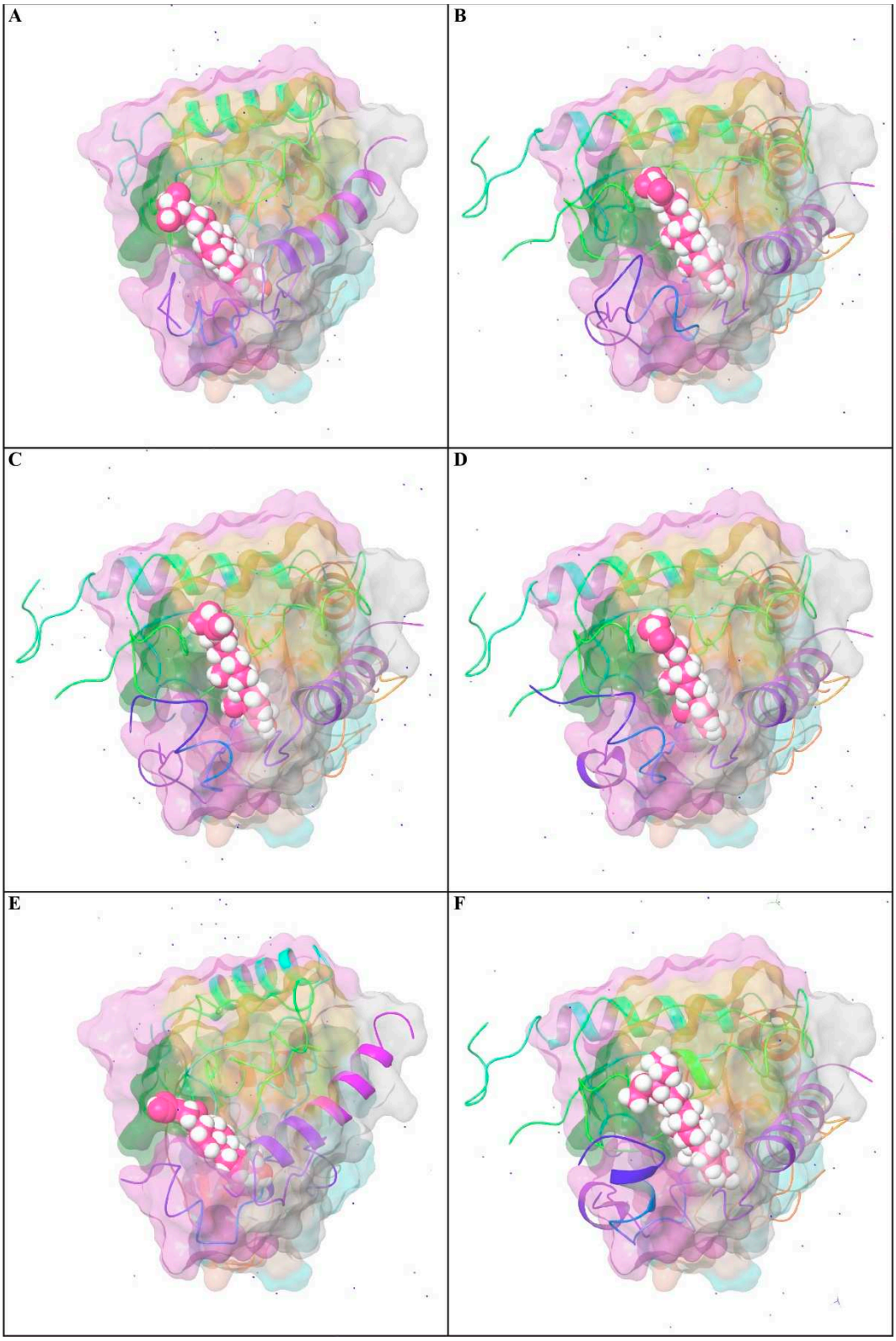

 doi:10.20944/preprints202306.0819.v1

Figure 10. The position of a ligand inside the pocket side during the selected trajectory (during the 75.00 to 100.00 ns). (A) at 75 ns, (B) at 80 ns, (C) at 85 ns, (D) at 90 ns, (E) at 95 ns, (F) at 100 ns.

MD-Movie-Frame_75
-1001_Clipchamp.mp4

Video 1: The video shows molecular dynamics simulations of the whole protein-ligand complex under *in vivo* mimic conditions.
https://drive.google.com/file/d/1UefhKZrJk1APbYLW8cPWazeCONILLsle/view?usp=share_link.

3.9.1. Protein root mean square deviation (P-RMSD)

The P-RMSD was used to calculate the difference in a protein's backbones from its initial structural conformation to its final position. The deviations induced during the simulation of the protein can be used to estimate its stability [26]. It was computed for each frame of the trajectory. **Figure 9A**, left Y-axis, demonstrates a protein's RMSD evolution. All protein frames were first aligned on the reference frame backbone before calculating the RMSD based on atom selection. The results showed that the P-RMSD values of the protein-ligand complex were stable between 75.00 to 100.00 ns, with the highest value being 5.68 and the lowest value being around 4.52, showing that the system equilibrated during this period.

3.9.2. Ligand root mean square deviation (L-RMSD)

L-RMSD (aligned on the ligand) demonstrates the ligand's stability (**Figure 9A**, right Y-axis). This RMSD value measures the internal fluctuations of the ligand atoms. 'Lig fit Lig' illustrates the RMSD of a ligand that has been aligned and assessed on only its reference conformation in this plot. During the MD simulation, the highest value of the L-RMSD was 1.69, while the lowest value was around 0.34.

3.9.3. Protein-Ligand contacts

Throughout the simulation, protein interactions with the ligand could well be observed. During the simulation, the stacked bar charts showed that the complex had H-bonds, hydrophobic interactions, and water bridges (**Figure 9B**). The number of individual connections produced by protein with the ligand throughout the selected trajectory (75.00 to 100.00 ns) was in the range of 0 to 7 contacts, according to a timeline depiction of the interactions and contacts (**Figure 9C**). Furthermore, the findings revealed that glutamic acid at protein residue position 389 (Glu389) was the protein residue that interacted with the ligands the most frequently (**Figure 9C**). A schematic of the precise ligand atom interactions with these protein residues was also shown in **Figure 9C**, right.

3.9.4. Position of a ligand inside the pocket side

The position of a ligand inside the pocket side during the MD simulation's equilibrated system (75.00 to 100.00 ns) is shown in **Figure 10** and **Video 1**. The snapshot of the protein-ligand complexes every five ns illustrated that the ligand was located at the same pocked site **(Figure** 2). The interactions and behavior of the ligand inside the pocket side during this equilibrated system were displayed in **Video 1**.

4. Discussion

The results of the present study reveal the antihypertensive effect of the extract of ripened sour *T. indica* (FRiST), the flesh of raw sour *T. indica* (FRaST), the flesh of ripened sweet *T. indica* (FSwT), and seeds of sour *T. indica* (SRiST) and their cooperative analysis on normal and cholesterol-induced hypertensive rats in a dose-dependent fashion. A cholesterol-rich diet and high-fat diets are linked to dyslipidemia which is considered a major risk factor for hypertension.

Polyphenols are a group of bioactive compounds having more than 7000 chemical entities present in different cereals, fruits, and vegetables. These natural compounds, impact over the total phenolic and flavonoid content as well as total antioxidant capacity, possess many OH groups which are largely responsible for their strong antioxidative, and anti-hypersensitive properties [27]. Polyphenols have attracted scientific interest for their beneficial effects in preventing oxidative stress-induced endothelial dysfunction through increasing eNOS activity reflected to scavenge ROS, inhibit NADPH and xanthine oxidases, and chelate metals which altogether increase the NO bioavailability, with an antihypertensive effect [28]. The proanthocyanidins, the largest and most ubiquitous plant polyphenolics, are reported to serve as novel antihypertensive therapy by modulating the cardiovascular disease risk markers, such as blood pressure and blood lipids [29–31]. Based on existing research, the antihypertensive effect of polyphenolic content is related to the activation of the nitric oxide system [32], the regulation of the endothelial function, and the inhibition of angiotensin I-converting enzyme (ACE) activity [33] required for the therapeutic intervention to control CVD-associated hypertension. Fernandez et al. have evaluated the effects of polyphenolic contents on ACE and shown that they could significantly inhibit the activity of ACE and NADPH oxidase, which might be one of the potential cardioprotective mechanisms [34,35]. Our study showed the highest presence of polyphenolic contents in FRaST aqueous extracts while other prior studies revealed higher polyphenolic contents in FRiST. However, further investigation might need for the quantitative polyphenolic estimation in methanolic extracts of FRiST, FRaST, FSwT, and SRiST, to evaluate their ACE inhibition capacity. Polyphenolics may also indirectly influence blood pressure by modulating inflammation and oxidative stress to reduce more than one CVD risk factor evident in animal studies [36,37]. Previous studies have confirmed that polyphenolics can display anti-inflammatory effects by significantly downregulating the expression of TNF-α、MCP-1 and IL-6 in high-fat diet-fed mice. Kanamoto et al. found that PCs significantly inhibited the expression levels of TNF-α、MCP-1 and IL-6 in high-fat diet-fed mice [38,39]. Therefore, polyphenolic supplementation may be a useful treatment for hypertensive patients and a preventive measure for prehypertensive and healthy subjects [40]. Furthermore, bioflavonoids show vasodilator effects in isolated aortae stimulated with noradrenaline, KCl, or phorbol esters and these effects are independent of the presence of endothelium [41]. Thus, this direct vasodilator effect and antioxidant property might contribute to its antihypertensive effects observed in the present study. Further investigation should be needed to evaluate the antioxidant activity of the four sample water extracts [42].

High dietary cholesterol has been shown to increase plasma cholesterol and may speed up the development of aortic atherosclerosis [43]. Numerous studies have shown that lowering cholesterol with diet or medication can reduce morbidity and mortality from CVD in the future. Based on this, significant efforts have been undertaken to lower the risk of CVD through the control of cholesterol, therefore the therapeutic advantages of plant foods have been the subject of several, in-depth dietary research (Yokozawa T) [44]. A study by Shivshankar and Shyamala Devi reported that rats supplemented with 10% *T. indica* pulp aqueous extract demonstrated a significantly reduced body weight after 2 weeks of treatment. The hypocholesterolemic effects of *T. indica* pulp fruit extracts have also been reported in 2006 by Martinello et al. [45]. Tamarind extract administration with cholesterol is found to inhibit the gaining of body weight in all extract groups except SRiST100. When compared to NC and PC, FRiST50 and FRaST50 significantly reduced body weight, confirming prior findings.

The crucial risk factor for CVD includes a low level of HDL-cholesterol which plays a direct role in the atherogenic process and a low level of HDL-cholesterol and increased risk of CVD is well established [46]. In the present study, apart from weight-reducing ability, aqueous extracts supplementation was observed to significantly decrease the levels of total cholesterol, total TG and LDL, and increase the HDL level by more than 50% in the plasma of the treatment group, which reversed the effect of high-fat diet consumption alone. The elevation of HDL concentration was found to be in a dose-dependent manner, where the group treated with FRaST 100 showed the highest increment, followed by FRiST extracts at 100 mg/kg and FSwT extracts at 100 mg/kg. Similar results were obtained by Martinello et al. [47]. The increase of HDL may be explained by the counteracting

 doi:10.20944/preprints202306.0819.v1

LDL oxidation, promoting the reverse cholesterol transport pathway by inducing an efflux of excess accumulated cellular cholesterol or by transition metal ion-based inhibition of LDL oxidation [48].

A dose-dependent administration of aqueous tamarind extracts also provided a beneficial effect on the reduction of total cholesterol, triglycerides, LDL-cholesterol, and VLDL cholesterol. The lipid-lowering potential of the extract may be attributed to the presence of phytochemical constituents like flavonoids, saponins, and tannins [49,50]. Flavonoids are reported to decrease LDL-cholesterol and increase HDL-cholesterol concentrations in hypercholesteraemic animals [51]. Saponins are reported to inhibit pancreatic lipase activity in high-fat diet-fed mice leading to greater fat excretion due to reduced intestinal absorption of dietary fats [49]. In this experiment, FRiST50 of the experimental group was found to be better for minimizing TC, TG, and LDL and the enriched content of flavonoids have a positive impact on this action.

An interrelationship between the functional integrity of the liver and the development and maintenance of hypertension is being increasingly recognised [49]. An absence of experimental and clinical hypertension with liver disease has been noted [52]. Alanine aminotransferase and aspartate aminotransferase, respectively localized in the hepatocellular cytosol and mitochondria, are the most specific markers of hepatic injury [53]. In the present study, the hepatic enzymes (ALT and AST) were significantly lower in antihypertensive treatment groups except in FRaST50, FSwT50, FRiST100, and SRiST100 groups which reflect a dose-dependent regulation of hypertension in the rat model. The serum level of ALP was higher in antihypertensive subjects than in the normotensive animal in a dose-dependent fashion. When variety and parts of Tamarindus were considered, elevated ALP levels were more likely to be found in the cholesterol-induced hypertensive rate of FRiST50, FRaST50, FSwT50, FRaST100, FSwT100 groups are at low risk of hypertension. A high prevalence of elevated levels of ALT and GGT demonstrated a higher risk for hypertensive females and males than their normotensive counterparts. A similar result was found in a previous study that reported a high prevalence of elevated ALT in the hypertensive group compared to the normotensive group [54]. There is no simple explanation for why a serum ALT showed an independent association with hypertension in the Bangladeshi population. One possibility may be that hypertensive individuals develop non-alcoholic fatty liver disease (NAFLD) after a long period of elevated blood pressure [55]. The postulated mechanism could be that increased blood pressure activates pro-inflammatory responses such as TNF-α and interleukin adiponectin and leptin that contribute to hepatotoxicity [56]. In parallel, oxidative stress is documented to be associated with hypertension [57] and antioxidant enzyme gene polymorphisms, including a few of the glutathione-S-transferase genes, have been reported to be correlated with the risk of hypertension in general adults [58,59].

The activity of the gluconeogenic enzyme, glucose-6- phosphatase, is usually enhanced during diabetes. After extract administration, blood glucose levels drop while the amount of liver glycogen increases. This may be due to the mobilization of blood glucose into the liver glycogen reserve [60,61]. Ramsay in 1977 discovered that 15% of experimental male hypertensive patients had abnormal liver function tests, suggesting a link between abnormal liver function tests and hypertension [62]. Animal models have also suggested a potential role for angiotensin II in the progression of NAFLD to hepatic fibrosis [63], and the use of angiotensin II type 1 receptor antagonists has been shown to reduce this progression [64]. The high liver glycogen level in cholesterol-induced hypertensive rats may be due to either increase in gluconeogenesis or hyperglycemia due to 18 h fasting before testing. In this study, in all treated groups except FRaST50, the reversion of the liver glycogen towards normal may be due to its activating effect on glucokinase and glycogen synthetase.

The C-reactive protein (CRP), a prototypical acute-phase reactant, is one of the most widely known biomarkers of cardiovascular disease. Circulating levels of CRP are clinically used to predict the occurrence of cardiovascular events and to aid in the selection of therapies based on more accurate risk assessment in individuals who are at intermediate risk. Hypertension has a positive correlation with CRP level. Cholesterol administration elevated CRP level. Antihypertensive drug and extract administration along with cholesterol lowered CRP level. Extract group of sweet *T. indica* (FSwT100),

ripen sour *T. indica* (FRiST50), and raw *T. indica* (FRaST100) significantly decreased CRP levels compared to NC and PC [65].

Previous studies suggested that chronic subclinical myocardial damage, detected by elevated Troponin I level, may precede the development of hypertension in the general population and that this novel biomarker of cardiac damage may have utility for identifying people at future risk for hypertension and hypertensive end-organ damage [66]. In addition, histopathology of cardiomyocytes was also performed to corroborate the findings of the biochemical investigation [67]. Our study also ameliorates the previous finding that myocardial damage along with troponin I level elevation is carried out synergistically. The tissue architecture of histopathological analysis reflected the partial amelioration of different cardiac sections changed through the hypertension-producing treatment. Histopathological observations showed less damage in the tamarind extract-treated group than the cholesterol-induced group and sometimes it is better than the positive control. Histopathological examinations revealed less damage in the tamarind extract-treated group compared to the cholesterol-induced group, and occasionally it was even better than the positive control [68]. As a result, it can be stated that the *Tamarindus indica* extract is highly effective in preventing cholesterol-induced hypertension in rats. Histopathological analysis of heart myocyte and troponin I level detection revealed that myocyte disruption, and myofibril infiltration appeared in the SRiST100 group, meanwhile, troponin I significantly elevated compared to other extracts and control groups. Further study is needed to reveal the composition difference of SRiST extract among other extract groups. In the present study, the findings in the cardiac tissues were found to be lesser in the FRiST group compared to the PC group. *T. indica* is enriched with antioxidant compounds like flavonoids, and vitamins C and E [69]. The antioxidant activity of the extract, which occurs through its free-radical scavenging activity, may have prevented oxidative damage at the myocardium in cholesterol-induced hypertensive rats. Furthermore, the antioxidant activity of quercetin contributed to *T. indica* extract would be helpful to manage glucose uptake and the glucose-induced increased levels of mitochondrial reactive oxygen species (ROS) linked to hyperglycemia [64]. The results of the present study showed that treatment with *T. indica* extract decreased cardiac damage in cholesterol-induced hypertensive rats except for SRiST100.

Oxidative reactions play an important role in plaque progression and instability, and the oxidation of LDL is the main event in the pathogenesis of atherosclerosis. Iron-dependent LDL may become critical when the progression of atheroma towards end-stage plaques leads to the liberation of iron ions, which mediate LDL oxidation by GSH hydrolysis production. In our study, we found a few compounds that are directly related to the antihypertensive activity. Among them compounds, a potentially useful zwitterionic buffer in the physiological pH range (6.0–8.5) is a novel class of glycylglycine amides that has been discovered to have value as antiarrhythmic agents [70]. Additionally, glycylclycine was reported to work as an acceptor in the catabolism of GGT that is raised in serum in cardiovascular (CV) mortality [71]. Among others, decanoic acid, 3-methyl- is reported to display antihypertensive activity through its antioxidant and anti-inflammatory action [72].

Molecular docking analyses are widely used to explore ligand-target interactions to identify the appropriate drug target for therapeutic innovation. It sheds more light on the likely methods of action and binding manner of various proteins' binding pockets [73]. Molecular docking in our study was used to further verify the antihypertensive action of T. indica through its ten lead compounds. The compounds were docked against eight targeted receptors described in the methodology section. Among the compounds, Gamma-sitosterol had the strongest binding interactions. The title compounds' anti-heart failure action could be mediated via binding or inhibiting Tyrosine Hydroxylase, BETA-1 subunit of guanylyl cyclase, BK channel, AT1 receptor antagonist, AT1 receptor antagonist combination with PPAR agonist, Thermolysin, Macrocyclic IL-17A antagonists and Human soluble guanylate cyclase. However, gamma-sitosterol has shown the best binding efficacy with the soluble guanylyl cyclase (GC-1) receptor which supports vascular function by catalyzing the conversion of GTP to cGMP via the NO/GC-1/cGMP pathway [74]. The cGMP stimulates protein kinase G, which phosphorylates a variety of substrates to cause vasodilation and prevention of platelet aggregation and adherence to the artery wall, among other actions.

 doi:10.20944/preprints202306.0819.v1

Dysfunction in the NO/GC-1/cGMP pathway has been linked to several vascular disorders via reactive oxygen species (ROS) [75].

The process of drug development requires toxicity assessment of novel compounds [76]. The pharmacokinetic properties of *T. indica* phytocompounds were tested by Lipinski's rule of five, which states that orally administered drugs should have a molecular weight ≤ 500 amu, Hydrogen bond acceptor sites ≤ 10, Hydrogen bond donor sites ≤ 5, and Lipophilicity value, Log P ≤ 4.15 and Veber's rule of two (number of rotatable bonds ≤ 10, topological polar surface area ≤ 140). The violation of these rules by any drug or phytoconstituent will lead to disqualifying its oral bioavailability as a good drug. Gamma-sitosterol of *T. indica* demonstrated the worthiest toxicokinetics ensuring its good oral bioavailability. Preclinical toxicity testing of GCMS compounds was studied in this work utilizing the admetSAR online server, and the results showed that all compounds are nontoxic and noncarcinogenic.

Network pharmacology (NP), which uses computational power to systematically catalogue the molecular interactions of a drug molecule in a living cell, is an emerging attempt to understand drug actions and interactions with multiple targets [77]. Protei-protein interaction (PPI) revealed possible target of identified compounds from the extract which are correlated with hypertension related pathways. The CYP17A1 is an enzyme that contributes to the synthesis of the hormones cortisol and aldosterone, which are important for controlling blood pressure. Studies have revealed that *CYP17A1* gene variants may be linked to elevated blood pressure and a higher risk of hypertension [78]. Aldosterone-mediated regulation of blood pressure is mediated by the mineralocorticoid receptor, which is encoded by the NR3C2 gene. According to studies, specific *NR3C2* gene variants may have a role in the emergence of hypertension [79]. The *VEGF* receptor 2, which is involved in controlling blood vessels, is encoded by the *KDR* gene. Blood pressure and the likelihood of developing hypertension have both been linked to higher *KDR* expression [80]. The *NOS2* gene is relevant for the nitric oxide-producing inducible nitric oxide synthase (iNOS) enzyme. Nitric oxide aids in blood pressure control and blood vessel relaxation. Blood pressure and hypertension have been linked to NOS2 deficiency [81]. The protein tyrosine phosphatase gene *PTPN1* modulates blood vessel tone, which in turn regulates blood pressure. According to studies, PTPN1 gene variants may have a role in the emergence of hypertension [82]. The JAK2 gene encodes a protein that participates in signaling pathways that control blood pressure. According to studies, there may be a link between JAK2 gene variants and an increased risk of hypertension [65]. The COX-2 enzyme, which is essential for the generation of prostaglandins, is encoded by the PTGS2 gene. Changes in prostaglandin levels can contribute to the development of hypertension as prostaglandins regulate blood pressure [66]. Renin, an enzyme involved in the control of blood pressure and fluid balance, is encoded by the gene REN. Renin expression has been associated with elevated blood pressure and a higher risk of hypertension [67]. HSD11B1 is an enzyme that participates in the metabolism of the hormone cortisol, which can have an impact on blood pressure. According to studies, hypertension risk may be increased by polymorphisms in the HSD11B1 gene [83]. Aldosterone, a hormone that controls blood pressure, is produced by the enzyme CYP11B2 in the body. According to studies, people who have CYP11B2 gene variants may be at a higher risk of getting hypertension [84]. A gene called PPARG encodes a protein that controls insulin sensitivity and blood pressure. According to studies, hypertension risk may be increased by polymorphisms in the PPARG gene [85].

The emergence and progression of hypertension have been linked to the genes HIF1A, CYP11B1, and NR3C1. The hypoxia-inducible factor 1 (HIF1A) gene controls how much oxygen is present in the body. This gene's impact on blood pressure control and angiogenesis has been found to contribute to the onset of hypertension and cardiovascular disease [86]. The gene CYP11B1 encodes a cytochrome P450 enzyme that is necessary for the manufacture of hormones, notably the stress hormone cortisol. Through its impact on cortisol levels, which can affect blood pressure regulation, this gene has been associated with hypertension [87]. The glucocorticoid receptor, a crucial regulator of the stress response and cortisol levels, is encoded by the nuclear receptor subfamily 3 group C member 1 (NR3C1) gene. Studies have revealed that NR3C1 polymorphisms can affect blood

 doi:10.20944/preprints202306.0819.v1

pressure regulation and cardiovascular function, and variations in this gene have been linked to an increased risk of hypertension [88].

It's crucial to keep in mind that although these genes have been linked to the control of blood pressure and the onset of hypertension, the relationship is complicated and may be altered by several variables, including a person's lifestyle and environment. To fully comprehend how these genes contribute to hypertension, more investigation is required.

Several genes, including *CYP17A1*, *CYP11B2*, *HSD11B1*, *CYP11B1*, and *NR3C2*, which are implicated in the control of hypertension, regulate the synthesis of steroid hormones, such as glucocorticoids, mineralocorticoids, androgens, and estrogens. Blood pressure can be influenced by the number of steroid hormones generated, and differences in the expression of these genes have been linked to a higher risk of hypertension [89]. Leishmaniasis has been connected to the emergence of hypertension and cardiac disease. Leishmaniasis is a parasite disease. The parasite's impact on the immune system, which can cause inflammation and alterations in blood pressure, is probably to blame for this. Numerous genes, including *PTPN1* and *NOS2*, have been linked to the emergence of hypertension in leishmaniasis patients [90,91]. The ovaries play a role in the synthesis of estrogen and other hormones, and differences in the expression of ovarian steroidogenesis genes, like *CYP17A1* and *CYP11B2*, have been linked to a higher risk of hypertension [92]. Additionally, the *HSD11B1* gene has been linked to the control of blood pressure and estrogen levels. The VEGF signaling pathway is connected to hypertension and is involved in the control of angiogenesis, and the formation of new blood vessels. Variations in how this pathway's genes, including KDR, are expressed have been linked to a higher risk of hypertension [93]. Cortisol, a glucocorticoid hormone, controls blood pressure and the body's reaction to stress. Several genes, including *CYP11B2*, *NR3C2*, and *HSD11B1*, control the synthesis and secretion of cortisol. Variations in the expression of genes implicated in this system, such as PRL, have been linked to an increased risk of hypertension. This pathway is important in the control of breastfeeding and hormone synthesis [94]. Resistance mechanisms to EGFR tyrosine kinase inhibitors: EGFR tyrosine kinase inhibitors are a class of cancer therapies that focus on the epidermal growth factor receptor. Changes in several genes, including *JAK2*, *PTGS2*, and *HIF1A*, which have also been connected to the emergence of hypertension, have been linked to resistance to these inhibitors. Gamma-sitosterol, a phytosterol, resembles cholesterol. Phytosterols may lower cholesterol, improve cardiovascular health, and reduce the incidence of some cancers. Angiotensin regulates blood pressure and fluid balance. It affects angiotensin receptors. Both AT1 and AT2 receptors regulate blood pressure and fluid balance [95]. Gamma-sitosterol and angiotensin receptors are poorly explored. Gamma-sitosterol may alter angiotensin receptor activation, which may improve blood pressure and cardiovascular health. Research on the relationship between gamma-sitosterol and thermolysin is scarce. Thermolysin is one of the proteases that may be able to be inhibited by phytosterols, particularly gamma-sitosterol, according to certain studies [95]. Potential therapeutic advantages of thermolysin and other protease inhibition include the treatment of cardiovascular disease, cancer, and inflammation.

Studies using MD simulations are thought to be useful for determining the relative stability and dynamic properties of ligand-target complexes. Additionally, MD simulations are more effective than static images produced by molecular docking and mechanical energy minimization technique for studying the complicated conformation space [97,98]. In the present study, we explored the binding affinity-based biological stability of the drug-likely antihypertensive molecules from *T. indica* to macromolecular receptors such as receptors Tyrosine Hydroxylase (PDB ID: 1TOH), BETA-1 subunit of the soluble guanylyl cyclase (PDB ID: 3HLS), Human High-conductance Ca^{2+} gated K^{+} Channel (BK Channel)(PDB ID: 3NAF), Nuclear hormone receptor PPAR-gamma(PDB ID: 3R8A), Human Angiotensin Receptor (PDB ID: 4YAY), Macrocyclic IL-17A antagonists (PDB ID: 5HI3), Human soluble guanylate cyclase (PDB ID: 6JT0). In our molecular simulation study, gamma-sitosterol was found to be a common bioactive molecule interacting with the majority of the selected target proteins especially guanylate cyclase which showed the lowest ligand RMSDs values than those of their respective proteins. The dynamic behaviors of ligand-complex confirm significant ligand/pocket accommodation, successful complex stability, and MD simulation convergence [99]. The protein's

collective dynamic motion/behavior was examined from MD simulation trajectories as part of further validation and monitoring of MD simulation convergence. Gamma-sitosterol's conformational stability at the guanylate cyclase, as determined by active site, MD modeling, supports the substance's potential for use as a medication.

Conclusion

This research has focused on the antihypertensive potential of different varieties of tamarinds while the sour type of tamarinds displayed the best effect in an animal model. Nonetheless, all tamarind varieties may be useful and beneficial as supplement or nutraceuticals for hypertensive patients. Future studies may approach the therapeutic transformation of tamarind to hypertension through further extensive and target-based study. Molecular docking, network-pharmacological analysis and molecular dynamic simulation validated the study with consistent evidence while pure isolated compounds from tamarinds would have been more impactful to affirm the biological potential of tamarinds in hypertension via elucidating the pure target ligand-receptor interaction.

CRediT authors statement: Taslima Akter: Data curation, Methodology, Data Analysis, Draft preparation; **Rakibul Hassan Bulbul** – Data curation, Methodology, Data Analysis, Draft preparation; **Imran Sama-ae** –Software, Data curation, **Md. Ali Azadi** – Methodology, Data Curation, **Kamrun Nahar Nira** - Methodology, Data Curation, **Salahuddin Quader Al-Araby** – Visualization and Validation Methodology, Data Curation; **Jobaier Ibne Deen**– Methodology, Data Curation; **Md. Khalid Juhani Rafi**: Software, Data curation, Methodology; **Srabonti Saha**–Validation, Reviewing, Visualization; **Md. Muzahid Ahmed Ezaj**–Methodology, Data curation; **Md Atiar Rahman**: Conceptualization, Data interpretation, Funding, Manuscript Reviewing and Editing. All the authors have gone through the manuscript and agreed to submit to the special issue of **"Foods".**

Funding: The authors received no funding for this study. Individual attempts and efforts led to the project being a success.

Data availability: All data are included in this manuscript. Raw data may be available on request.

Acknowledgment: The authors wish to thank the members of the Laboratory of Alternative Medicine and natural products research for their extensive cooperation in accomplishing the research.

Conflicts of Interest: The authors declare that they don't have any conflict of interest.

List of Abbreviations

C-reactive protein-CRP
White blood cell-WBC
Lactate Dehydrogenase-LDL
High-density lipoprotein-HDL
Normal control group-NC
Positive control group-PC
Total cholesterol-TC
Triglyceride-TG
Low-density lipoprotein-LDL
Very low-density lipoprotein-VLDL
Serum Aspartate Aminotransferase-AST
Alanine Aminotransferase-ALT
Alkaline phosphatase-ALP
Gallic acid equivalents-GAE
Hypertension-HTN
Total Phenolic Content-TPC
Total Flavonoid Content-TFC
Flesh of Ripen Sour Tamarind = FRiST
Seed of Ripen Sour Tamarind = SRiST
Flesh of Raw Sour Tamarind = FRaST
Flesh of Sweet Tamarind = FSwT

References

1. Cotran KC. Cellular Pathology. Robbins Pathologic basis of disease. Fifth Ed 1999.
2. Corless JK, Middleton HM. Normal liver function: a basis for understanding hepatic disease. Arch Intern Med 1983;143:2291–4.
3. Rahman S, Islam S, Haque T. Association between serum liver enzymes and hypertension: a cross-sectional study in Bangladeshi adults. BMC Cardiovasc Disord 2020;20:128. https://doi.org/10.1186/s12872-020-01411-6—12.
4. Ernesto L, Schifrin R, M T. Heart and Circulatory Physiology. Am J Physiol 2004;287.
5. Nandave M, K OS, S AD. Protective role of flavonoids in cardiovascular disease. Rev Artic Nat Prod Radiance 2005;4:166–76.
6. Sies H. Oxidative stress: oxidants and antioxidant. Exp Physiol 1997;82:291–5.
7. Prieto P, Pineda M, Aguilar M. Spectrophotometric quantitation of antioxidant capacity through the formation of a phosphomolybdenum complex: specific application to the determination of Vitamin E 1999.
8. Kala CP. Indigenous uses, population density, and conservation of threatened medicinal plants in protected areas of the Indian Himalayas. Conserv Biol 2005;Apr;19(2):368-78.
9. Kumaran A, Karunakaran RJ. In vitro antioxidant activities of methanol extracts of five Phyllanthus species from India. LWT-Food Sci Technol 2007;40:344–52.
10. Akter H, Rashid MM, Islam MS, Hossen MA, Rahman MA, Algheshairy RM, et al. Biometabolites of Tamarindus indica play a remarkable cardioprotective role as a functional food in doxorubicin-induced cardiotoxicity models. J Funct Foods 2022;96:105212.
11. RincónC, MontoyaJ, GómezG. Optimizing the extraction of phenolic compounds from *Bixa orellana* L. and effect of physicochemical conditions on its antioxidant activity. *J* Med Plant Res. 2014;8(46):1333-1339.
12. Singleton VL, Rossi JA. Colorimetry of total phenolics with phosphomolybdic-phosphotungstic acid reagents. Am J Enol Viticult 1965;16:144–58.
13. Abdelseed BH, Abdalla AH, AE GA, A AMI. Some Nutritional Attributes of Selected Newly Developed Lines of Sorghum (Sorghum bicolor) after Fermentation. J Agr Sci Tech 2011;13:399–409.
14. Lo S, Russell JC, Taylor AW. Determination of glycogen in small tissue samples. J Appl Phys 1970;28:234–6.
15. Alam S, Nasreen S, Ahmad A, Darokar MP, Khan F. Detection of natural inhibitors against human liver cancer cell lines through QSAR, molecular docking and ADMET studies. Curr Top Med Chem 2021;21:686–95.
16. Aksoydan B, Kantarcioglu I, Erol I, Salmas RE, Durdagi S. Structure-based design of hERG-neutral antihypertensive oxazalone and imidazolone derivatives. J Mol Graph Model 2018;79:103–17.
17. Casimiro-Garcia A, Filzen GF, Flynn D, Bigge CF, Chen J, Davis JA, et al. Discovery of a series of imidazo [4, 5-b] pyridines with dual activity at angiotensin II type 1 receptor and peroxisome proliferator-activated receptor-γ. J Med Chem 2011;54:4219–33.
18. Hussein HA, Borrel A, Geneix C, Petitjean M, Regad L, Camproux A-C. PockDrug-Server: a new web server for predicting pocket druggability on holo and apo proteins. Nucleic Acids Res 2015;43:W436–42.
19. Hussain J, Rehman N, Al-Harrasi A, Ali L, Ullah R, Mabood F. Nutritional prospects and mineral compositions of selected vegetables from Dhoda sharif – Kohat. J Med Plant Res 2011.
20. Lipinski CA, Lombardo F, Dominy BW, Feeney PJ. Experimental and computational approaches to estimate solubility and permeability in drug discovery and development settings. Adv Drug Deliv Rev 1997;23:3–25.
21. Veber DF, Johnson SR, Cheng H-Y, Smith BR, Ward KW, Kopple KD. Molecular properties that influence the oral bioavailability of drug candidates. J Med Chem 2002;45:2615–23.
22. Yang H, Lou C, Sun L, Li J, Cai Y, Wang Z, et al. admetSAR 2.0: web-service for prediction and optimization of chemical ADMET properties. Bioinformatics 2019;35:1067–9.
23. Shaw DE, Adams PJ, Azaria A, Bank JA, Batson B, Bell A, et al. Anton 3: twenty microseconds of molecular dynamics simulation before lunch. Proc. Int. Conf. High Perform. Comput. Netw. Storage Anal., 2021, p. 1–11.
24. Thangavel N, Al Bratty M, Al Hazmi HA, Najmi A, Ali Alaqi RO. Molecular docking and molecular dynamics aided virtual search of OliveNet™ directory for secoiridoids to combat SARS-CoV-2 infection and associated hyperinflammatory responses. Front Mol Biosci 2021;7:627767.

25. Sukati S, Sama-ae I, Katzenmeier G, Wisessombat S. Evaluation of Susceptibility of the Human Pathogen Helicobacter pylori to the Antibiotic Capreomycin. Sci World J 2022;2022.
26. Aier I, Varadwaj PK, Raj U. Structural insights into conformational stability of both wild-type and mutant EZH2 receptor. Sci Rep 2016;6:1–10.
27. Das M, Devi KP, Belwal T, Devkota HP, Tewari D, Sahebnasagh A, et al. Harnessing polyphenol power by targeting eNOS for vascular diseases. Crit Rev Food Sci Nutr 2021:1–26.
28. Curin Y, Andriantsitohaina R. Polyphenols as potential therapeutical agents against cardiovascular diseases. Pharmacol Rep 2005;57:97.
29. Singh R, Singh S, Kumar S, Arora S. Evaluation of antioxidant potential of ethyl acetate extract/fractions of Acacia auriculiformis A. Cunn Food Chem Toxicol 2007;45:1216–23.
30. Graf BL, Raskin I, Cefalu WT, Ribnicky DM. Plant-derived therapeutics for the treatment of metabolic syndrome Curr Opin Investig Drugs 2010;11:1107–15.
31. Feringa HHH, Laskey DA, Dickson JE, C.I. Coleman The effect of grape seed extract on cardiovascular risk markers: a meta-analysis of randomized controlled trials Am Diet Assoc 2011;111:1173–81.
32. Fisher NDL, Hughes M, Gerhard-Herman M, N.K. Hollenberg Flavanol-rich cocoa induces nitric-oxide-dependent vasodilation in healthy humans Hypertens 2003;21:2281–6.
33. Fernández K, J. Labra Simulated digestion of proanthocyanidins in grape skin and seed extracts and the effects of digestion on the angiotensin I-converting enzyme (ACE. Inhib Act Food Chem 2013;139:196–202.
34. Ottaviani JI, Actis-Goretta L, Villordo JJ, C.G. Fraga Procyanidin structure defines the extent and specificity of angiotensin I converting enzyme inhibition Biochimie 2006;88:3–4.
35. Pons Z, Guerrero L, Margalef M, Arola L, Arola-Arnal A, B. Muguerza Effect of low molecular grape seed proanthocyanidins on blood pressure and lipid homeostasis in cafeteria diet-fed rats. J Physiol Biochem 2014;70:629–37.
36. Terra X, Palozza P, Fernandez J, Larrea A, Ardevol C, Blade G, et al. Blay Procyanidin dimer B1 and trimer C1 impair inflammatory response signalling in human monocytes. Free Radic Res 2011;45:611–9.
37. Bourvellec CL, Boas PBV, Lepercq P, Comtet S, Marre PA, Ruiz P, et al. Mosoni Procyanidin-Cell Wall Interactions within Apple Matrices Decrease the Metabolization of Procyanidins by the Human Gut Microbiota and the Anti-Inflammatory Effect of the Resulting Microbial Metabolome In Vitro Nutrients 2019;11:664.
38. Kanamoto Y, Yamashita Y, Nanba F, Yoshida T, Tsuda T, Fukuda I, et al. Ashida A black soybean seed coat extract prevents obesity and glucose intolerance by up-regulating uncoupling proteins and down-regulating inflammatory cytokines in high-fat diet-fed mice J. Agric Food Chem 2011;59:8985–93.
39. Ren J, An J, Chen M, Yang H, Ma Y. Effect of proanthocyanidins on blood pressure: A systematic review and meta-analysis of randomized controlled trials, Pharmacological Research,Volume 165,2021,105329,ISSN 1043-6618 n.d.
40. Duarte J, Pérez-Vizcaíno F, Utrilla MP, Jiménez J, Tamargo J, Zarzuelo A. Vasodilatory effects of flavonoids in rat aortic smooth muscle. Struct-Act Relatsh Gen Pharmacol 1993;24:857–64.
41. Hollman PCH, Trijp JMP, Buysman MNCP, Gaag MS, Mengelers MJB, Vries JHM, et al. Relative bioavalability of the antioxidant flavonoid quercetin from various foods in man. FEBS Lett 1997;418:152–6.
42. Stanley J. Dietary cholesterol, blood cholesterol and cardiovascular disease. Lipid Technol 2010;22:110–2.
43. Vinué Á, Herrero-Cervera A, González-Navarro H. Understanding the impact of dietary cholesterol on chronic metabolic diseases through studies in rodent models. Nutrients 2018;10:939.
44. Shivshankar P, Shyamala Devi CS. Evaluation of costimulatory effects of Tamarindus indica L. on MNU-induced colonic cell proliferation. Food Chem Toxicol 2004;42:1237–44.
45. Martinello F, Soares SM, Franco JJ, Santos AC, Sugohara A, Garcia SB, et al. Hypolipemic and antioxidant activities from Tamarindus indica L. pulp fruit extract in hypercholesterolemic hamsters. Food Chem Toxicol 2006;44:810–8. https://doi.org/10.1016/j.fct.2005.10.011.
46. Assmann G, Gotto Jr AM. HDL cholesterol and protective factors in atherosclerosis. Circulation 2004;109:III-8-III–14.
47. Kolawole OT, Kolawole SO, Ayankunle AA, Olaniran OI. Methanol leaf extract of Persea americana protects rats against cholesterol-induced hyperlipidemia. Br J Med Med Res 2012;2:235–42.
48. Yokozawa T, Cho EJ, Sasaki S, Satoh A, Okamoto T, Sei Y. The protective role of Chinese prescription Kangen-karyu extract on diet-induced hypercholesterolemia in rats. Biol Pharm Bull 2006;29:760–5.

49. Music M, Dervisevic A, Pepic E, Lepara O, Fajkic A, Ascic-Buturovic B. Metabolic syndrome and serum liver enzymes level at patients with type 2 diabetes mellitus. Med Arch 2015;69.
50. Vernon G, Baranova A, Younossi Z. Systematic review: the epidemiology and natural history of non-alcoholic fatty liver disease and non-alcoholic steatohepatitis in adults. Aliment Pharmacol Ther 2011;34:274–85.
51. Han SH, Nicholls SJ, Sakuma I, Zhao D, Koh KK. Hypertriglyceridemia and Cardiovascular Diseases: Revisited. Korean Circ J 2016.
52. Hong ZF, Zhao WX, Yin ZY, Xie CR, Xu YP, Chi XQ. Capsaicin Enhances the Drug Sensitivity of Cholangiocarcinoma through the Inhibition of Chemotherapeutic-Induced Autophagy. PloS One 2015;10.
53. López-Suárez A, Guerrero JMR, Elvira-González J, Beltrán-Robles M, Cañas-Hormigo F, Bascuñana-Quirell A. Nonalcoholic fatty liver disease is associated with blood pressure in hypertensive and nonhypertensive individuals from the general population with normal levels of alanine aminotransferase. Eur J Gastroenterol Hepatol 2011;23:1011–7.
54. Eslami S, Sahebkar A. Glutathione-S-transferase M1 and T1 null genotypes are associated with hypertension risk: a systematic review and meta-analysis of 12 studies. Curr Hypertens Rep 2014;16.
55. Musso G, Gambino R, Michieli F, Durazzo M, Pagano G, Cassader M. Adiponectin gene polymorphisms modulate acute adiponectin response to dietary fat: possible pathogenetic role in NASH. Hepatol Balt Md 2008;47:1167–77.
56. Touyz RM. Reactive oxygen species, vascular oxidative stress, and redox signaling in hypertension: what is the clinical significance? Hypertension 2004;44:248–52.
57. Mansego ML, Solar GDM, Alonso MP, Martínez F, Sáez GT, Escudero JCM. Polymorphisms of antioxidant enzymes, blood pressure and risk of hypertension. J Hypertens 2011;29:492–500.
58. Sachdewa A, Khemani LD. Effect of Hibiscus rosasinensis L ethanol flower extract on blood glucose and lipid profile in streptozotocin- induced diabetes in rats. J Ethnopharmacol 2003;89:61–6.
59. SB K, KG P. Histological structure of pancreas in normal control, diabetic control and extract treated Albino rats. Int J Life Sci 2016;4:78–82.
60. Hage FG. C-reactive protein and hypertension 2014;28:410–5.
61. Lemos JA, Drazner MH, Omland T, Ayers CR, Khera A, Rohatgi A, et al. Association of troponin T detected with a highly sensitive assay and cardiac structure and mortality risk in the general population. JAMA 2010;304:2503–12. https://doi.org/10.1001/jama.2010.1768.
62. Yokohama S, Yoneda M, Haneda M, Okamoto S, Okada M, K A. Therapeutic efficacy of an angiotensin II receptor antagonist in patients with nonalcoholic steatohepatitis. Hepatology 2004;40:1222–5.
63. Azab HA, El-Nady AM, Hamed MA, Ahmed IT. Potentiometric determination of the dissociation constants of glycylglycine in various aquo-organic media. J Chin Chem Soc 1995:42,769-77.
64. Usa K, Liu Y, Geurts AM, Cheng Y, Lazar J, Baker MA, et al. The antihyperlipidemic effect of N. sativa seed extract may be attributed to the synergistic effect of its different constituents, soluble fiber, sterols, flavenoids and high content of polyunsaturated fatty acids n.d.
65. Milara J, Ballester B, Morell A, Ortiz JL, Escrivá J, Fernández E, et al. JAK2 mediates lung fibrosis, pulmonary vascular remodelling and hypertension in idiopathic pulmonary fibrosis: an experimental study. Thorax 2018;73:519–29.
66. Ross S, Eikelboom J, Anand SS, Eriksson N, Gerstein HC, Mehta S, et al. Association of cyclooxygenase-2 genetic variant with cardiovascular disease. Eur Heart J 2014;35:2242–8.
67. Smyth LJ, Cañadas-Garre M, Cappa RC, Maxwell AP, McKnight AJ. Genetic associations between genes in the renin-angiotensin-aldosterone system and renal disease: A systematic review and meta-analysis. BMJ Open 2019;9:e026777.
68. Mukherjee S, Banerjee SK, Maulik M, Dinda AK, Talwar KK, Maulik SK. Protection against acute adriamycin-induced cardiotoxicity by garlic: role of endogenous antioxidants and inhibition of TNF-α expression. BMC Pharmacol 2003;3:1–9.
69. Berg AH, Drechsler C, Wenger J, Buccafusca R, Hod T, Kalim S, et al. Carbamylation of serum albumin as a risk factor for mortality in patients with kidney failure. Sci Transl Med 2013;6;5(175):175ra29. https://doi.org/10.1126/scitranslmed.3005218.
70. Lindberg UHA, Akerman SBA. Novel glycylglycine amides. Google Patents; 1975.
71. Yoshiji H, Kuriyama S, Yoshii J, Ikenaka Y, Noguchi R, T N. Angiotensin-II type 1 receptor interaction is a major regulator for liver fibrosis development in rats. Hepatology 2001;34:745–50.

72. Ramsay LE. Liver dysfunction in hypertension. Lancet 1977;2:111–4.
73. Pinzi L, Rastelli G. Molecular docking: shifting paradigms in drug discovery. Int J Mol Sci 2019;20:4331.
74. Derbyshire ER, Marletta MA. Structure and regulation of soluble guanylate cyclase. Annu Rev Biochem 2012;81:533–59.
75. Buys ES, Potter LR, Pasquale LR, Ksander BR. Regulation of intraocular pressure by soluble and membrane guanylate cyclases and their role in glaucoma. Front Mol Neurosci 2014;7:38.
76. Andrade EL, Bento AF, Cavalli J, Oliveira SK, Schwanke RC, Siqueira JM, et al. Non-clinical studies in the process of new drug development-Part II: Good laboratory practice, metabolism, pharmacokinetics, safety and dose translation to clinical studies. Braz J Med Biol Res 2016;49.
77. Hopkins AL. Network pharmacology: the next paradigm in drug discovery. Nat Chem Biol 2008.
78. Li Q, Gao T, Yuan Y, Wu Y, Huang Q, Xie F, et al. Association of CYP17A1 genetic polymorphisms and susceptibility to essential hypertension in the southwest Han Chinese population. Med Sci Monit Int Med J Exp Clin Res 2017;23:2488.
79. van Dijk EH, Schellevis RL, van Bergen MG, Breukink MB, Altay L, Scholz P, et al. Association of a haplotype in the NR3C2 gene, encoding the mineralocorticoid receptor, with chronic central serous chorioretinopathy. JAMA Ophthalmol 2017;135:446–51.
80. Wang Y, Zheng Y, Zhang W, Yu H, Lou K, Zhang Y, et al. Polymorphisms of KDR gene are associated with coronary heart disease. J Am Coll Cardiol 2007;50:760–7.
81. Xie X, Shi X, Xun X, Rao L. Endothelial nitric oxide synthase gene single nucleotide polymorphisms and the risk of hypertension: a meta-analysis involving 63,258 subjects. Clin Exp Hypertens 2017;39:175–82.
82. Chistiakov DA, Voronova NV, Chistiakova EI. Identification of new susceptibility genes for type 1 diabetes: an update. Curr Immunol Rev 2008;4:116–33.
83. Rahman T, Avery PJ, Mayosi BM, Watkins H, Keavney B. Association between HSD11B1 polymorphism and left ventricular mass in families with hypertension. BMJ Publishing Group Ltd and British Cardiovascular Society; 2009.
84. Li W, Liu C. The− 344C/T polymorphism in the CYP11B2 gene is associated with essential hypertension in the Chinese. J Renin Angiotensin Aldosterone Syst 2014;15:150–5.
85. Zhang M, Zhang J, Li L, Wang Q, Feng L. Association between peroxisome proliferator-activated receptor γ-2 gene Pro12Ala polymorphisms and risk of hypertension: an updated meta-analysis. Biosci Rep 2019;39.
86. Smith KA, Waypa GB, Dudley VJ, Budinger GS, Abdala-Valencia H, Bartom E, et al. Role of hypoxia-inducible factors in regulating right ventricular function and remodeling during chronic hypoxia–induced pulmonary hypertension. Am J Respir Cell Mol Biol 2020;63:652–64.
87. Kosicka K, Siemiątkowska A, Szpera-Goździewicz A, Krzyścin M, Bręborowicz GH, Główka FK. Increased cortisol metabolism in women with pregnancy-related hypertension. Endocrine 2018;61:125–33.
88. Patel GC, Liu Y, Millar JC, Clark AF. Glucocorticoid receptor GRβ regulates glucocorticoid-induced ocular hypertension in mice. Sci Rep 2018;8:1–13.
89. Hakhoe TS, Hakhoe TY, Health NI of. The Korean journal of physiology & pharmacology: official journal of the Korean Physiological Society and the Korean Society of Pharmacology. 1997.
90. Prasad R, Singh UK, Mishra OP, Jaiswal BP, Muthusami S. Portal hypertension with visceral leishmaniasis. Indian Pediatr 2010;47:965–7.
91. Yu Y-D, Hou W-J, Zhang J, Xue Y-T, Li Y. Network pharmacology and molecular docking-based analysis on bioactive anticoronary heart disease compounds in Trichosanthes kirilowii maxim and bulbus allii macrostemi. Evid Based Complement Alternat Med 2021;2021.
92. Bentley-Lewis R, Seely E, Dunaif A. Ovarian hypertension: polycystic ovary syndrome. Endocrinol Metab Clin 2011;40:433–49.
93. Lankhorst S, Saleh L, Danser AJ, van den Meiracker AH. Etiology of angiogenesis inhibition-related hypertension. Curr Opin Pharmacol 2015;21:7–13.
94. Brooks K, Burns G, Spencer TE. Biological roles of hydroxysteroid (11-beta) dehydrogenase 1 (HSD11B1), HSD11B2, and glucocorticoid receptor (NR3C1) in sheep conceptus elongation. Biol Reprod 2015;93:38, 1–12.
95. Yadegari M, Sellami M, Riahy S, Mirdar S, Hamidian G, Saeidi A, et al. Supplementation of Adiantum capillus-veneris modulates alveolar apoptosis under hypoxia condition in Wistar rats exposed to exercise. Medicina (Mex) 2019;55:401.

96. Reguengo LM, Salgaço MK, Sivieri K, Júnior MRM. Agro-industrial by-products: Valuable sources of bioactive compounds. Food Res Int 2022;152:110871.
97. Karplus M, Petsko GA. Molecular dynamics simulations in biology. Nature 1990;347:631–9.
98. Selvaraj C, Sakkiah S, Tong W, Hong H. Molecular dynamics simulations and applications in computational toxicology and nanotoxicology. Food Chem Toxicol 2018;112:495–506.
99. Elhady SS, Abdelhameed RF, Malatani RT, Alahdal AM, Bogari HA, Almalki AJ, et al. Molecular docking and dynamics simulation study of hyrtios erectus isolated scalarane sesterterpenes as potential SARS-CoV-2 dual target inhibitors. Biology 2021;10:389.